

# Perspectives of 2D MXene Tribology

Andreas Rosenkranz,\* Maria Clelia Righi,\* Anirudha V. Sumant,\* Babak Anasori,\*  
and Vadym N. Mochalin\*

The large and rapidly growing family of 2D early transition metal carbides, nitrides, and carbonitrides (MXenes) raises significant interest in the materials science and chemistry of materials communities. Discovered a little more than a decade ago, MXenes have already demonstrated outstanding potential in various applications ranging from energy storage to biology and medicine. The past two years have witnessed increased experimental and theoretical efforts toward studying MXenes' mechanical and tribological properties when used as lubricant additives, reinforcement phases in composites, or solid lubricant coatings. Although research on the understanding of the friction and wear performance of MXenes under dry and lubricated conditions is still in its early stages, it has experienced rapid growth due to the excellent mechanical properties and chemical reactivities offered by MXenes that make them adaptable to being combined with other materials, thus boosting their tribological performance. In this perspective, the most promising results in the area of MXene tribology are summarized, future important problems to be pursued further are outlined, and methodological recommendations that could be useful for experts as well as newcomers to MXenes research, in particular, to the emerging area of MXene tribology, are provided.

efficiency, the significance of tribology becomes evident in light of global challenges such as decreasing earth resources, i.e., fossil fuel and minerals, as well as steadily rising CO<sub>2</sub> emissions contributing to global warming.<sup>[4,5]</sup> In this context, friction and wear have been identified as notably contributing toward a downgraded energy efficiency, inviting the development of greener, smarter, and more sustainable tribological processes and lubricants.

Since ancient times, the most straightforward approach to reduce friction and wear was to place a liquid lubricant (oil or grease) between the rubbing surfaces. This greatly reduces or eliminates the solid–solid contact, thus enabling low-friction and low-wear conditions.<sup>[6]</sup> However, after centuries of use, liquid lubricants have been pushed toward their limits due to the current trend of continuously reducing the lubricant viscosity and, therefore, the resulting film thickness. This, in turn, increases the amount of solid–solid contact, leading to

harsher tribological conditions with increased friction and wear. Combined with more stringent regulations regarding the use of sulfur- and phosphorous-containing lubricant additives as well as efforts toward decarbonization to reduce CO<sub>2</sub> emissions and hazardous wastes, these factors propel the urgent development of alternative lubrication concepts.<sup>[4]</sup>

In this context, nanomaterials used as additives in base oils or applied as solid lubricant coatings have gained notable

## 1. Introduction

Tribology, which covers friction, wear, and lubrication, is essential for the proper functioning of bearings, piston rings, and gears, among others.<sup>[1]</sup> Besides engineering applications, it connects with broader aspects of our daily life ranging from consuming food and beverages<sup>[2]</sup> to wearing contact lenses and cosmetics.<sup>[3]</sup> Due to its direct connection to energy and fuel

A. Rosenkranz  
Department of Chemical Engineering, Biotechnology and Materials  
FCFM  
University of Chile  
Santiago 7820436, Chile  
E-mail: arosenkranz@ing.uchile.cl


M. C. Righi  
Department of Physics and Astronomy  
University of Bologna  
Bologna 40127, Italy  
E-mail: clelia.righi@unibo.it

A. V. Sumant  
Center for Nanoscale Materials  
Argonne National Laboratory  
Lemont, IL 60439, USA  
E-mail: sumant@anl.gov

B. Anasori  
Department of Mechanical and Energy Engineering  
Purdue School of Engineering and Technology and Integrated Nanosystems  
Development Institute  
Indiana University-Purdue University Indianapolis  
Indianapolis, IN 46202, USA  
E-mail: banasori@iupui.edu

V. N. Mochalin  
Department of Chemistry  
Missouri University of Science and Technology  
Rolla, MO 65409, USA  
E-mail: mochalinv@mst.edu

V. N. Mochalin  
Department of Materials Science and Engineering  
Missouri University of Science and Technology  
Rolla, MO 65409, USA

 The ORCID identification number(s) for the author(s) of this article can be found under <https://doi.org/10.1002/adma.202207757>.

DOI: 10.1002/adma.202207757

attention.<sup>[7–10]</sup> Irrespective of the tribological conditions (dry or lubricated), they can reduce friction and/or wear by changing the underlying friction mode (sliding versus rolling friction) due to their low-shear strength or the ability to form beneficial tribofilms.<sup>[7,8,11]</sup> The use of nanomaterials in tribology has been boosted by the discovery of graphene and its derivatives with their outstanding friction and wear performance.<sup>[12]</sup> Afterward, significant progress has been made using transition metal dichalcogenides (TMDCs) such as MoS<sub>2</sub> and WS<sub>2</sub> in their 2D forms as solid lubricants.<sup>[7,13–15]</sup> Since each nanomaterial brings its own material-specific advantages and limitations, the tribological community continuously explored new nanomaterials with enhanced tribological properties optimized for specific working conditions.

Over the past decade, the materials science community has become increasingly interested in MXenes, a large family of 2D transition metal carbides, nitrides, and carbonitrides with the chemical formula M<sub>n+1</sub>X<sub>n</sub>T<sub>x</sub> (n = 1 to 4). In this chemical formula, M represents a 3d–5d transition metal and X is either C or N bonded to M in an octahedral configuration.<sup>[16,17]</sup> Unlike their bulk counterparts, 2D MXene flakes expose the majority of their M atoms on the surface. The surface transition metal atoms are terminated with a mixture of –O, –F, –OH, or –Cl, collectively indicated by T (terminations) in the MXene formula. Since the stoichiometric ratio of the surface terminations depends on the environment,<sup>[18]</sup> the formula<sup>[17]</sup> shows it as x in T<sub>x</sub>, where x is unknown but is, in many cases, close to 2 (Figure 1a).

MXenes are synthesized from ternary and quaternary carbide and nitride precursors (mostly MAX phases)<sup>[19]</sup> by selective topochemical removal of the A layers (an A-group element, commonly from groups 13–16 of the Periodic Table), usually in aqueous hydrofluoric acid<sup>[20,21]</sup> or molten salt etchants,<sup>[22]</sup> where the etching environment defines the composition and type of T in the resultant MXene.<sup>[18,23,24]</sup> A wide array of compositional, structural, and processing choices permits the application-driven design of MXenes.<sup>[17,25,26]</sup> Among known 2D materials, MXenes offer a unique combination of properties: high mechanical stiffness (330–450 GPa for a monolayer<sup>[27]</sup>) and high 2D flake bending rigidity,<sup>[28]</sup> combined with high electrical conductivity<sup>[29]</sup> and hydrophilicity.<sup>[21]</sup> Due to their hydrophilicity and high negative zeta potential (approximately –30

to –50 mV), 2D MXene flakes can be easily dispersed in water and polar liquids.<sup>[30]</sup> They demonstrate a strong affinity toward oppositely charged species,<sup>[31]</sup> which can help to bind MXenes to other 2D materials or bulk surfaces.

Nanometer-thick MXene monolayers can be stacked via interflake interactions, allowing for easy shearing and sliding within the stack. Moreover, the van der Waals and hydrogen bonds between MXenes result in 2–6 times stronger interflake interactions in MXene stacks as compared to graphite or MoS<sub>2</sub>.<sup>[32]</sup> The interlayer interaction energy depends on the respective surface terminations. Therefore, the control over intrinsic functional groups of MXenes (T), for example, lowering the strength of hydrogen bonding by reducing the extent of MXene hydroxylation, can provide unmatched opportunities to tune shear and sliding in a MXene stack. Similar to other layered materials, metal and non-metal cations, as well as small molecules (e.g., hydrazine or urea) can be intercalated into MXenes,<sup>[18,31]</sup> providing an additional control over the MXene interlayer spacing and, consequently, sliding and shearing within the stacks.<sup>[33]</sup> This opens up interesting opportunities in the area of nanotribology.<sup>[34,35]</sup>

The aforementioned combination of properties together with their chemical reactivity, which is essential to form beneficial tribofilms, make MXenes prospective materials for tribological applications under dry and lubricated conditions. The detailed understanding of their structure and fundamental physical as well as chemical properties is essential for the rational development of MXene applications. Consequently, we start with a brief overview of the most important features of MXene structure and chemistry. Afterward, we summarize the existing state-of-the-art of MXene tribology before addressing the current challenges and outlining future research directions.

## 2. Structure and Chemistry of MXenes

Chemically, MXenes are 2D forms of early transition metal carbides, nitrides, and carbonitrides in a mostly hexagonal-close-packed crystal lattice (P63/mmc space group) with an octahedral configuration of C or N around the transition metal atom (Figure 2a).<sup>[26]</sup> The MXene terminology, which classifies MXenes with different compositions as single M MXenes,

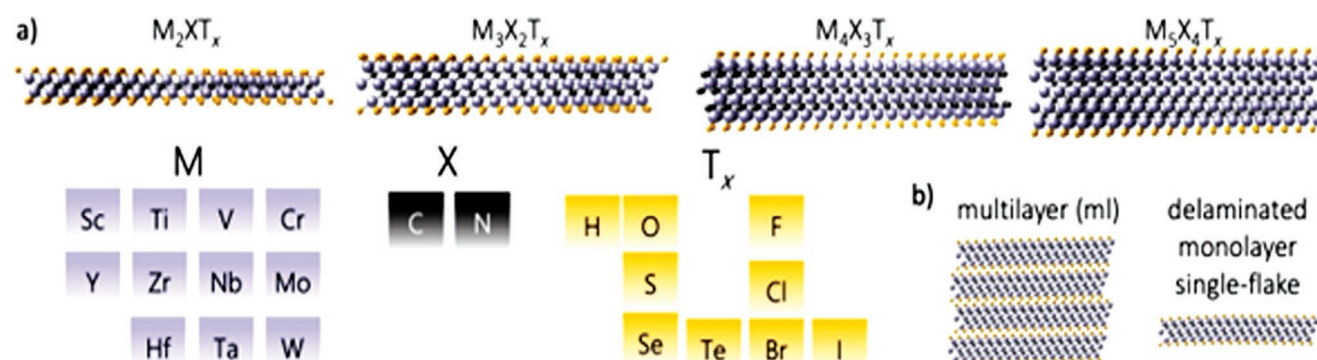


**Figure 1.** Chemical composition and structure of MXenes synthesized to date. a) Variability in the monolayer thicknesses of MXenes (top row shows archetypal structures of M<sub>2</sub>X<sub>1</sub>T<sub>x</sub>, M<sub>3</sub>X<sub>2</sub>T<sub>x</sub>, M<sub>4</sub>X<sub>3</sub>T<sub>x</sub>, and M<sub>5</sub>X<sub>4</sub>T<sub>x</sub>, which have different monolayer thicknesses with n ranging from 1 to 4), and their elemental composition in terms of M, X, and T (bottom row). b) Schematics of the multilayer and delaminated MXenes (also called single-flake or monolayer MXenes).

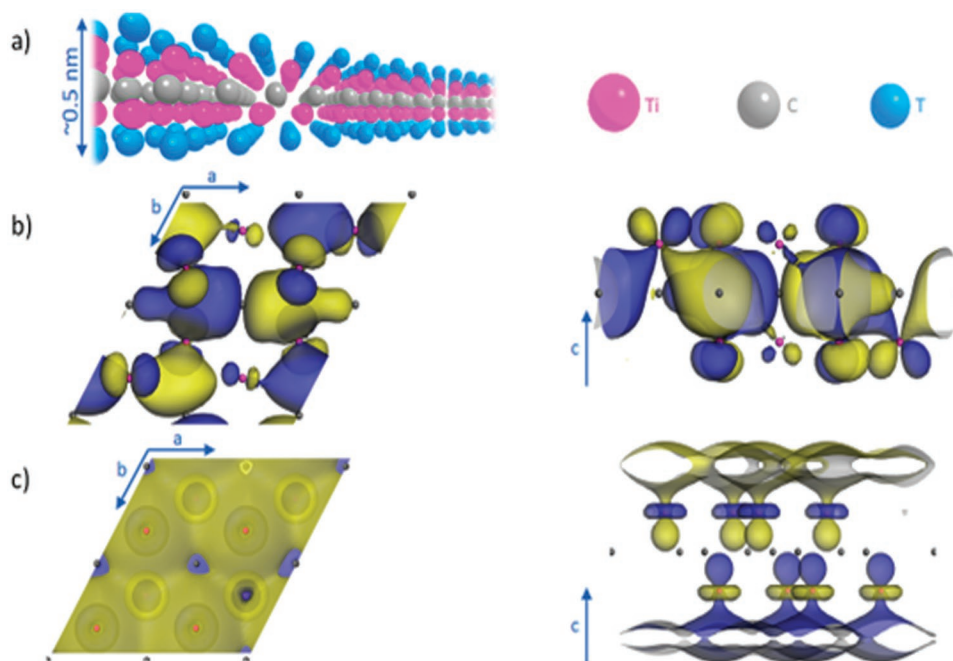


**Figure 2.** Structure of Ti<sub>2</sub>C MXene. a) A monolayer of Ti<sub>2</sub>C MXene is shown terminated by the functional groups T with  $x = 2$ . b) Top (left) and side (right) views of one of the bonding molecular orbitals (blue and yellow colors correspond to different signs of the wavefunction) of bare Ti<sub>2</sub>C, mainly formed by the overlap of the hybridized  $e_g$  orbitals of Ti atoms with the  $sp^3$  orbitals of the C atoms, leading to strong M–X covalent bonds within the MXene monolayer. c) Top (left) and side (right) views of the HOMO orbital of bare Ti<sub>2</sub>C mainly formed by the overlap of the  $e_g$  orbitals of the Ti atoms, creating regions of high electron density on both sides of the MXene layer, which makes it susceptible to electrophilic attack, leading to surface terminations. The colors of the elements adopted in this figure are shown in the legend in the top right.

double M random solid solution, and ordered M in- and out-of-plane ordered MXenes (i-MXenes and o-MXenes), and multilayer (ml-MXenes) versus delaminated (d-MXenes) (Figure 1b), has been reviewed elsewhere.<sup>[16]</sup> Splitting of d orbitals of M in the octahedral ligand field leads to a twofold degenerated  $e_g$  ( $d_{z^2}$  and  $d_{x^2-y^2}$ ) and a threefold degenerated  $t_{2g}$  ( $d_{xy}$ ,  $d_{yz}$ , and  $d_{xz}$ ) energy levels. The splitting magnitude is less in lower symmetries, which implies that the  $e_g$  and  $t_{2g}$  energies in MXenes are closer than in their corresponding bulk carbides. The hybridized  $e_g sp^3_{x,y,z}$  orbitals of M form strong directional  $\sigma$  bonds with the s and p orbitals of X (Figure 2b), while the  $t_{2g}$  orbitals of M, directed between the  $\sigma$  bonds, overlap with the p orbitals of X leading to weaker  $\pi$  bonds.<sup>[36]</sup> In addition to M–X bonds, a long-range overlap between the  $t_{2g}$  orbitals of the neighboring M atoms leads to  $\sigma'$  M–M molecular orbitals, which are antibonding in character.

The HOMO orbital in bare MXenes is exposed on both sides of the bare MXene monolayers (Figure 2c), rendering them particularly susceptible to the attack by electrophiles, which explains the ease with which surface terminations T are attached to all experimentally produced MXenes. The partially ionic character of M–X bonds decreases with an increase in the number of d electrons in M. For a given M, the ionic character of the M–X bonds decreases in the following order: M oxide > M nitride > M carbide. Since the ionic character of the bonds correlates with the material's bandgap, MXenes are more electrically conductive than the corresponding M oxides. In this context, carbide MXenes are more conductive than nitride MXenes of the same M element. The X–X distances in MXenes are too long for appreciable electron overlap, and

the X–X bonding in MXenes is negligible. The M–X and M–T bonds are key in determining the mechanical properties of MXenes, as was reviewed elsewhere.<sup>[26]</sup>

MXene surface chemistry plays a pivotal role in tailoring their properties.<sup>[16,37]</sup> Their synthesis in aqueous environments always results in oxygen-containing T (–O–, –OH). In addition, commonly used fluorine-containing etchants introduce –F terminations. While the relative amounts of the F- and O-containing surface groups slightly vary depending on the synthesis conditions, precise control of the surface terminations using aqueous fluorine-based etchants is presently unachievable. Electrochemical<sup>[38]</sup> and hydrothermal<sup>[39]</sup> etching of MAX phases eliminates fluorine but still yields a random mixture of T (–O–, –OH, and –Cl). To avoid oxygen-containing functional groups and yield a more uniform surface chemistry, molten salt etching has been explored. Etching Ti<sub>3</sub>AlC<sub>2</sub> in molten ZnCl<sub>2</sub> and other Lewis acidic molten salts above 500 °C yields Ti<sub>3</sub>C<sub>2</sub>Cl<sub>2</sub> MXene.<sup>[22,40]</sup> A variant of this method is the synthesis of Ti<sub>3</sub>C<sub>2</sub>Cl<sub>2</sub>, Ti<sub>2</sub>CCL<sub>2</sub>, and Nb<sub>2</sub>CCL<sub>2</sub> MXenes in molten CdCl<sub>2</sub> (or Ti<sub>3</sub>C<sub>2</sub>Br<sub>2</sub> and Ti<sub>2</sub>CBr<sub>2</sub> in CdBr<sub>2</sub>, respectively), followed by a halogen exchange for S, Se, Te, or “vacancy” (□).<sup>[23]</sup> Although these techniques produce ml-MXenes with a better control of the resulting surface chemistry, their further delamination without exposure to water (which will reintroduce O-containing moieties) is challenging. As an alternative, direct reactions of the parental MAX phases with halogens in organic solvents have been explored to produce d-MXenes with T = –Br or –I.<sup>[41]</sup> Overall, the research area of MXene surface modification is still in its infancy, with only a handful of techniques reported, some of which need verification. Additionally,

intercalated species, for example, water, cations or small molecules, can play a role in the tribological behavior of MXenes. The intercalation chemistry of MXenes has been thoroughly reviewed recently.<sup>[42]</sup>

Regarding the chemical reactivity of MXenes with the environment, recent experiments have demonstrated that they can directly and completely react with water (hydrolysis) in ambient conditions,<sup>[43,44]</sup> which is quite unexpected, considering the textbook knowledge about the chemical inertness of bulk transition metal carbides exposed to water under these and even harsher conditions. Although there was at least one prior publication on the hydrolysis of bulk TiC in ambient conditions,<sup>[45]</sup> the reaction was limited by 5–30 surface atomic layers and was considered minor or negligible. Consequently, the reactivity of bulk transition metal carbides with water in ambient conditions has not received sufficient attention. However, the reactivity of MXenes with water in similar conditions cannot be ignored. The experimental observation of MXene hydrolysis invites more systematic studies on the reactivity of MXenes toward other substances and environments. It is important to understand MXene reactivity not only with the purpose of suppressing it, as in some cases, but understanding and harnessing the reactivity may be key for rational development of applications. For instance, chemical transformations of MXenes under wear conditions may yield beneficial tribofilms acting to dissipate friction energy and reduce wear.<sup>[46,47]</sup> Hence, not only the chemistry but also the tribochemistry of MXenes seem to be of interest for future research.

### 3. Tribology of MXenes

In the past two decades, numerous tribological studies with various 2D materials, including graphene and its derivatives, as well as TMDCs under different tribological conditions, have been published.<sup>[7,13–15]</sup> From the physics point of view, their beneficial friction performance was traced back to their lamellar structure with weak van der Waals forces acting between the layers.<sup>[15,26,48]</sup> These characteristics provide the layered materials with a considerably low shear strength, which results in low friction following the theory of Bowden and Tabor.<sup>[49]</sup> Moreover, the ability of 2D materials to stick to different surfaces<sup>[34,35,50,51]</sup> passivates the contacts, significantly decreasing interfacial adhesion. The formation of beneficial tribofilms and the reorientation of the basal planes parallel to the acting shear force have also been shown to contribute toward improved friction and wear characteristics.<sup>[46,52]</sup>

When selecting 2D materials for specific tribological applications/purposes, it is crucial to consider the entire tribological system (substrate and counterbody), the acting loads and kinematics, as well as the environmental conditions (atmosphere, temperature, and humidity).<sup>[13,26,53]</sup> In case of 2D materials, the common drawbacks observed so far are their inability to work at high contact pressures and sliding velocities and relatively poor adhesion when being drop-cast or spray-coated onto the base substrates. This implies that once these materials start to wear off, they tend to lose their functionality, resulting in catastrophic wear and notably increased friction.<sup>[15,46,54]</sup>

As with other 2D materials used in tribology, MXenes offer a 2D layered structure; however, they are distinct due to their theoretically predicted easy-to-shear ability, fair mechanical properties, excellent tunability (composition and surface chemistry), and reactivity.<sup>[26,55]</sup> As mentioned above, the chemical reactivity of MXenes can be an advantage considering their possible transformations with the formation of a tribolayer in conditions of high pressures and temperatures locally occurring in tribological contacts. Depending on the substrate and counterbody as well as the environment, the formation of beneficial oxides is possible, intermixed with chemically and structurally degraded MXenes. The in-situ-formed tribofilm tends to have a good substrate adhesion and may induce long-lasting low-friction and low-wear performance.<sup>[46,56]</sup> In oxygen- and water-free environments, MXenes are more stable at elevated temperatures. Their 2D layered structure can survive heating up to  $\approx 900$  °C in an inert atmosphere.<sup>[57]</sup> At higher temperatures, carbide MXenes are transformed into 3D crystalline bulk transition metal carbides,<sup>[58]</sup> for instance TiC, which are well-known hard materials. Moreover, MXene reactivity and chemical modification can be further exploited to combine them with other 2D materials such as graphene/graphene oxide (GO) or adjust their hydrophilicity to be more compatible with water- or oil-based lubricants.<sup>[26,51,59]</sup>

### 4. MXenes for Liquid Lubrication

When used as lubricant additives, some nanoparticles can act as nano-roller-bearings changing the underlying friction mode from sliding to rolling, thus reducing friction. Moreover, they can form beneficial tribofilms by reacting with the rubbing counterbody or substrate material, leading to low friction and enhanced wear performance.<sup>[9,10]</sup> Irrespective of the nanomaterial used as a lubricant additive, the success and possibility to reduce friction and wear greatly depend on the phase compatibility (nanomaterial and base oil) and dispersion stability. Only homogeneous, stable nanosheet/oil dispersions can result in robust friction and wear reduction. In contrast, unstable dispersions may form agglomerates over time, thus degrading the tribological performance due to increased abrasion and resistance against motion.<sup>[10,11,60,61]</sup>

In the past five years, MXenes have been used as additives to reduce friction and wear under lubricated conditions. In this regard, ml-<sup>[62–64]</sup> or d-Ti<sub>3</sub>C<sub>2</sub>T<sub>x</sub><sup>[65,66]</sup> have been mixed with non-additivated 100SN,<sup>[62]</sup> poly-(alpha)-olefin,<sup>[63]</sup> paraffin,<sup>[64]</sup> and castor base oil.<sup>[65]</sup> Hybrid TiO<sub>2</sub>- and potassium titanate-Ti<sub>3</sub>C<sub>2</sub>T<sub>x</sub> composites have also been utilized as additives in base oils.<sup>[67,68]</sup> Moreover, the lubrication performance of Ti<sub>3</sub>C<sub>2</sub>T<sub>x</sub> has been tested in glycerol,<sup>[69]</sup> ethylene glycol,<sup>[70]</sup> and distilled water.<sup>[71,72]</sup> Additionally, Nb<sub>2</sub>CT<sub>x</sub> has been recently tested in water lubrication,<sup>[73]</sup> while the lubrication performance of Mo<sub>2</sub>CT<sub>x</sub> has been studied in a lithium-based ionic liquid.<sup>[74]</sup> In pure base oils, Ti<sub>3</sub>C<sub>2</sub>T<sub>x</sub> and its hybrids have shown the best performance at concentrations  $\approx 1$  wt% leading to twofold friction and ninefold wear volume reductions.<sup>[62–66]</sup> Lower or higher concentrations of Ti<sub>3</sub>C<sub>2</sub>T<sub>x</sub> nanosheets induced less beneficial or even detrimental effects because of either insufficient amount of lubricious material (when MXene concentrations are below optimal)



or agglomeration at higher MXene concentrations.<sup>[26,55,69]</sup> The use of  $Ti_3C_2T_x$  nanosheets significantly reduced abrasion and deformation, resulting in a much smoother wear track. The improved tribological performance induced by  $Ti_3C_2T_x$  and its nanocomposites in base oils and other polar lubricants relates to the formation of MXene-rich, self-lubricating tribofilms induced by tribochemical reactions. The tribofilms typically consist of oxide species originating from the substrate and/or counterbody, which are intermixed with chemically and structurally degraded MXene nanosheets. It has been shown that the tribofilm formation starts at the onset of the tribological experiment and the best performance is achieved when forming a homogeneous and uniform tribofilm across the entire tribological contact. Subsequently, this tribofilm is transferred to the rubbing counterbody. This reduces direct contact between the surfaces, thus accommodating the energy dissipation processes in a tribofilm/tribofilm system. The tribofilms with easy-to-shear ability, originating due to the weak interflake interactions of the  $Ti_3C_2T_x$  nanosheets, further reduce friction and wear.<sup>[69,74,75]</sup>

The rather limited success of using MXenes as lubricant additives in pure base oils is related to their inherent hydrophilicity due to polar surface terminations, which limits their dispersion stability and induces agglomeration in non-polar media. However, MXene surface terminations also bear potential for chemical functionalization, which can be used to tailor the degree of hydrophobicity (oleophilicity). For instance, Feng et al. grafted tetradecylphosphonic acid onto ml- $Ti_3C_2T_x$  (Figure 3a), which notably improved its dispersion in castor oil and led to a 30% reduction in friction and a 55% reduction

in the wear rate (Figure 3b).<sup>[65]</sup> Recently, dialkyl dithiophosphate moieties were grafted onto tannic acid- $Fe^{3+}$  complex precoated  $Ti_3C_2T_x$  flakes.<sup>[76]</sup> This approach improved MXene dispersion in the base oils leading to a stable coefficient of friction (CoF) of 0.11, an 87% wear volume reduction, and a load-bearing capacity reaching 500 N. Guo et al. verified that poly[2-(perfluorooctyl)ethyl methacrylate]] (PPFMA)-grafted  $Ti_3C_2T_x$  (Figure 3c) showed an improved dispersibility in perfluoropolyether (PFPE) and, therefore, improved friction and wear performance (Figure 3d).<sup>[77]</sup> These studies exemplify the power of chemical functionalization to improve MXene dispersion in nonpolar liquids, leading to lower friction and wear under lubricated conditions.<sup>[65]</sup>

Apart from chemical functionalization, the formation of heterostructures is an effective way to improve the dispersion stability of MXenes in pure base oils, thus notably reducing friction and wear. Recently, this approach has been verified for d- $Ti_3C_2T_x$  forming self-dispersing heterostructures with  $MoS_2$ <sup>[78]</sup> and hydroxysalts<sup>[75]</sup> in mineral oil and PAO 10, respectively. In case of the d- $Ti_3C_2T_x/MoS_2$  heterostructure, friction and wear reductions of 39% and 85%, respectively, were demonstrated, while the d- $Ti_3C_2T_x$ /hydroxysalt heterostructure induced a stable CoF of 0.12 for contact pressures up to 3.28 GPa. In both cases, the improved dispersion stability of the heterostructures was explained by the reduced restacking tendency of MXenes due to nanosteric hindrance. This guaranteed a continuous supply of lubricious material to the contact zone, thus beneficially contributing to the formation of a homogeneous tribofilm with its subsequent transfer to the counterbody.<sup>[75,78]</sup>

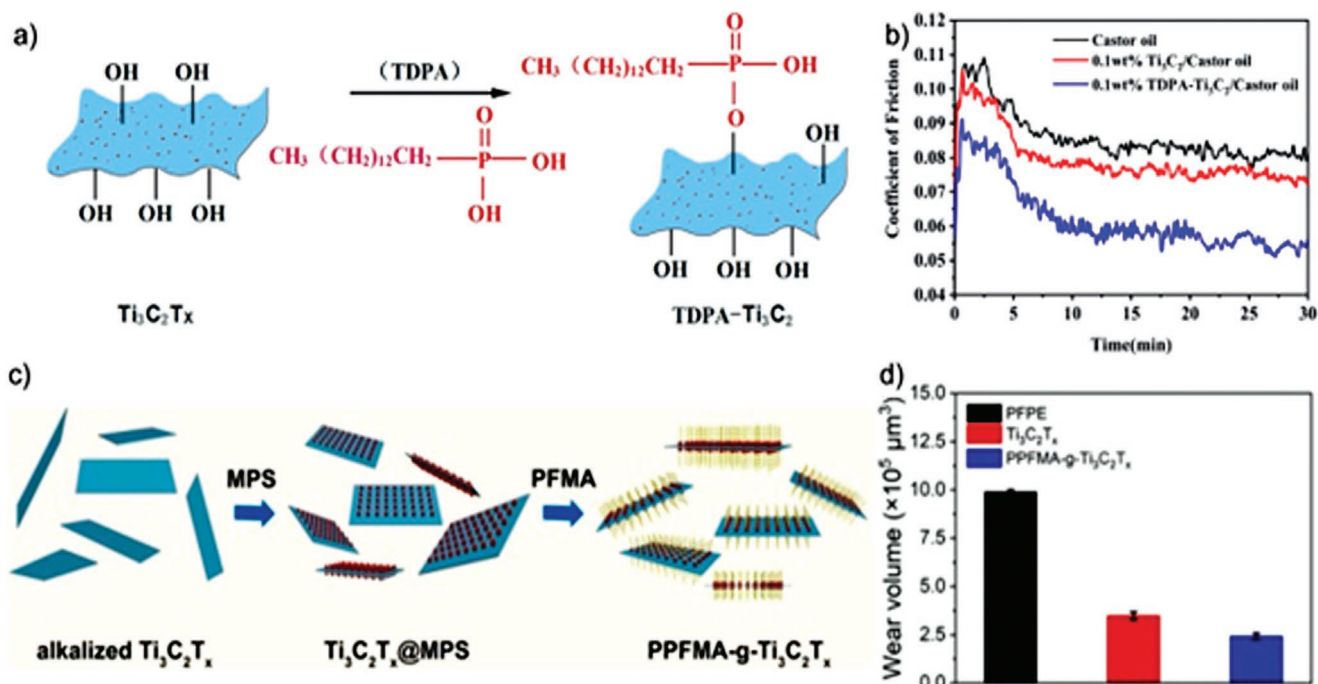


**Figure 3.** MXenes as lubricant additives: a) An approach to chemical functionalization of ml- $Ti_3C_2T_x$  using tetradecylphosphonic acid (TDPA) and b) temporal evolution of CoF comparing the tribological performance of pure castor oil to castor oil mixed with as-synthesized  $Ti_3C_2T_x$  and  $TDPA-Ti_3C_2T_x$ . a,b) Reproduced with permission.<sup>[65]</sup> Copyright 2021, Elsevier. c) Schematic illustration of the synthesis steps of poly[2-(perfluorooctyl)ethyl methacrylate]] (PPFMA) grafted  $Ti_3C_2T_x$  ( $PPFMA-g-Ti_3C_2T_x$ ) and d) comparison of the resulting wear volumes for perfluoropolyether (PFPE) without additives, pure  $Ti_3C_2T_x$  and  $PPFMA-g-Ti_3C_2T_x$  as additives. c,d) Reproduced with permission.<sup>[77]</sup> Copyright 2022, Elsevier.

Due to inherent hydrophilicity, ml-Ti<sub>3</sub>C<sub>2</sub>T<sub>x</sub><sup>[71,72]</sup> and ml-Nb<sub>2</sub>CT<sub>x</sub>, as well as moderately or completely oxidized Nb<sub>2</sub>CT<sub>x</sub> nanosheets,<sup>[73]</sup> have been used as additives in water. Nguyen et al. reported that low amounts of ml-Ti<sub>3</sub>C<sub>2</sub>T<sub>x</sub> nanosheets induced a 37% friction reduction and a twofold reduction in the wear rate.<sup>[71]</sup> Besides MXene high surface-to-volume ratio and hydrophilicity, the improved tribological properties were related to a tribolayer formation and its transfer to the counter body.<sup>[72]</sup> Partially oxidized ml-Nb<sub>2</sub>CT<sub>x</sub> in water (0.25 mg mL<sup>-1</sup>) reduced friction and wear rate by 90% and 73%, respectively. The formation of a relatively thick (>74 nm) tribofilm (consisting of Nb<sub>2</sub>C, Nb<sub>2</sub>O<sub>5</sub>, and carbon) transferred to the counterbody was confirmed by cross-sectional transmission electron microscopy images.<sup>[73]</sup> These initial studies of MXenes for water lubrication have shown an improved performance due to their better dispersibility and greater ability to form MXene-rich self-lubricating tribo-films. The studies also suggest the potential of higher quality, larger, and more stable MXene flakes as additives to further reduce wear under water lubrication.

The first experimental evidence of Ti<sub>3</sub>C<sub>2</sub>T<sub>x</sub> induced superlubricity (CoF < 0.01) in a liquid environment was obtained at Si<sub>3</sub>N<sub>4</sub>/sapphire interfaces, where 1 wt% of ml-Ti<sub>3</sub>C<sub>2</sub>T<sub>x</sub> in glycerol resulted in CoF ≈ 0.002, which remained stable over 3 h sliding time. The detailed characterization of the rubbing surfaces confirmed the formation of a 23 nm-thick tribofilm and its transfer to the Si<sub>3</sub>N<sub>4</sub> counterbody.<sup>[69]</sup> Subsequently, superlubricious states under considerably high contact pressures of up to 1.42 GPa have been verified for ml-Mo<sub>2</sub>CT<sub>x</sub> as additives in lithium-hexafluorophosphate-based ionic liquids with Si<sub>3</sub>N<sub>4</sub>/sapphire contacts.<sup>[74]</sup> A detailed chemical analysis of the formed tribofilms (substrate and counterface) demonstrated the formation of Mo<sub>x</sub>O<sub>y</sub> and P<sub>x</sub>O<sub>y</sub>, which were intermixed with aligned ml-Mo<sub>2</sub>CT<sub>x</sub> nanosheets. The formed oxide species are known to induce low-friction and anti-wear performance under harsher contact conditions (boundary lubrication). Together with the aligned nanosheets, which induce a low shear strength, this resulted in the establishment of superlubricious behavior over a broader range of experimental conditions.<sup>[74]</sup>

## 5. MXenes for Solid Lubrication

The usage of solid lubricant coatings in tribology greatly depends on the coating quality (homogeneity, surface roughness, and thickness) and the coating/substrate adhesion. Only homogeneous, well-adhered coatings can effectively and efficiently improve tribological performance. Approaches including drop-casting, spin-coating, and spray-coating, among others, are frequently used for coating deposition, which all require as an important prerequisite the formation of stable dispersions in different solvents,<sup>[26]</sup> emphasizing the importance of the fundamental understanding of MXene chemistry and physics and details of their interactions with different solvents.<sup>[30]</sup> As outlined above, MXene surface chemistry and hydrophilicity ensure good dispersibility in aqueous and polar organic solvents, which is crucial for the deposition of homogeneous solid lubricant coatings onto mainly solid substrates.

The past three years have witnessed a growing interest in using MXenes as solid lubricant coatings. Two main

approaches have been pursued: the use of neat solid Ti<sub>3</sub>C<sub>2</sub>T<sub>x</sub> or hybrid nanocomposites of Ti<sub>3</sub>C<sub>2</sub>T<sub>x</sub> with other nanomaterials. Regarding the first approach, ml-Ti<sub>3</sub>C<sub>2</sub>T<sub>x</sub> nanosheets have been deposited on different substrates including copper,<sup>[79]</sup> stainless steel,<sup>[46,80–82]</sup> and silicon<sup>[56,83]</sup> by spray-coating,<sup>[79,82]</sup> drop-casting,<sup>[80,81]</sup> and electro-spraying.<sup>[46]</sup> The resulting coating thickness varied from 100 nm<sup>[46]</sup> to several micrometers.<sup>[80]</sup> The tribological properties of these coatings were mainly studied in ball-on-disk tests using various counter-ball materials and contact pressures ranging from 300 MPa to 1.5 GPa. ml-Ti<sub>3</sub>C<sub>2</sub>T<sub>x</sub> coatings showed up to a fourfold friction reduction compared to uncoated reference systems.<sup>[79,81,82]</sup> A study evaluating the tribological performance of ml-Ti<sub>3</sub>C<sub>2</sub>T<sub>x</sub> coatings at different relative humidities revealed the best performance at low humidity, ≈20%.<sup>[80]</sup> Higher friction was observed for humidity ≈ 80%,<sup>[80]</sup> which correlates with MXene reactivity toward water.<sup>[43,51]</sup> A 100 nm-thick electrosprayed coating of neat ml-Ti<sub>3</sub>C<sub>2</sub>T<sub>x</sub> has shown outstanding wear resistance and durability (**Figure 4a,b**). This performance was traced back to the formation of a beneficial tribofilm containing a mixture of degraded MXenes as well as amorphous and nanocrystalline iron oxide (**Figure 4c,d**). The tribofilm was first formed on the substrate and then transferred to the counterbody. The electrosprayed MXene coatings demonstrated superior improvements in wear life as compared to other state-of-the-art solid lubricants (graphene, graphene oxide, MoS<sub>2</sub>) and their binary nanocomposites,<sup>[46]</sup> although at a much greater film thicknesses.

The first large-scale demonstration of the superlubricity of neat Ti<sub>3</sub>C<sub>2</sub>T<sub>x</sub> solid lubricant coatings was realized in a dry nitrogen environment (**Figure 4e,f**).<sup>[51]</sup> Furthermore, the combination of ml-Ti<sub>3</sub>C<sub>2</sub>T<sub>x</sub> with graphene preserved the superlubricity of MXene, while reducing the coating wear rate in dry N<sub>2</sub> at contact pressures up to 600 MPa.<sup>[51]</sup> In this case, the combined effect of passivating MXene by graphene (as previously seen for MoS<sub>2</sub>-graphene<sup>[84]</sup> and MoS<sub>2</sub>-graphene oxide composites<sup>[85]</sup>) as well as the incommensurability between MXene and graphene layers may have helped in extending the wear life and maintaining the superlubricity via easy shearing between MXene and graphene layers.<sup>[51]</sup> Moreover, Ti<sub>3</sub>C<sub>2</sub>T<sub>x</sub> nanosheets have been combined with different nanomaterials including nanodiamond<sup>[56]</sup> and quantum dots<sup>[83]</sup> on silicon substrates. Hybrid MXene-nanodiamond coatings have shown excellent wear resistance with almost zero wear.<sup>[56]</sup> This performance of pure and hybrid Ti<sub>3</sub>C<sub>2</sub>T<sub>x</sub> solid lubricant coatings was connected to the in situ formation of a beneficial tribofilm, initially on the substrate, with subsequent transfer to the counterbody.<sup>[46,83,86]</sup> This transforms the initial substrate/counterbody system into a tribofilm/tribofilm system with different friction properties (**Figure 4c,d,g,h**). All frictional processes in the newly formed tribofilm/tribofilm interface benefit from the easy-to-shear ability of the nanosheets and the advantageous mechanochemical properties of the tribofilm.

**Table 1** compares the solid lubrication performance of different neat 2D nanomaterials (including Ti<sub>3</sub>C<sub>2</sub>T<sub>x</sub>) and their combinations. For a fair comparison, we limited the scope to studies performed without any chemical functionalization of the 2D materials. Similarly, we have not included vacuum and inert gas conditions (although beneficial for some 2D materials) since the state-of-the-art of MXene tribology does not

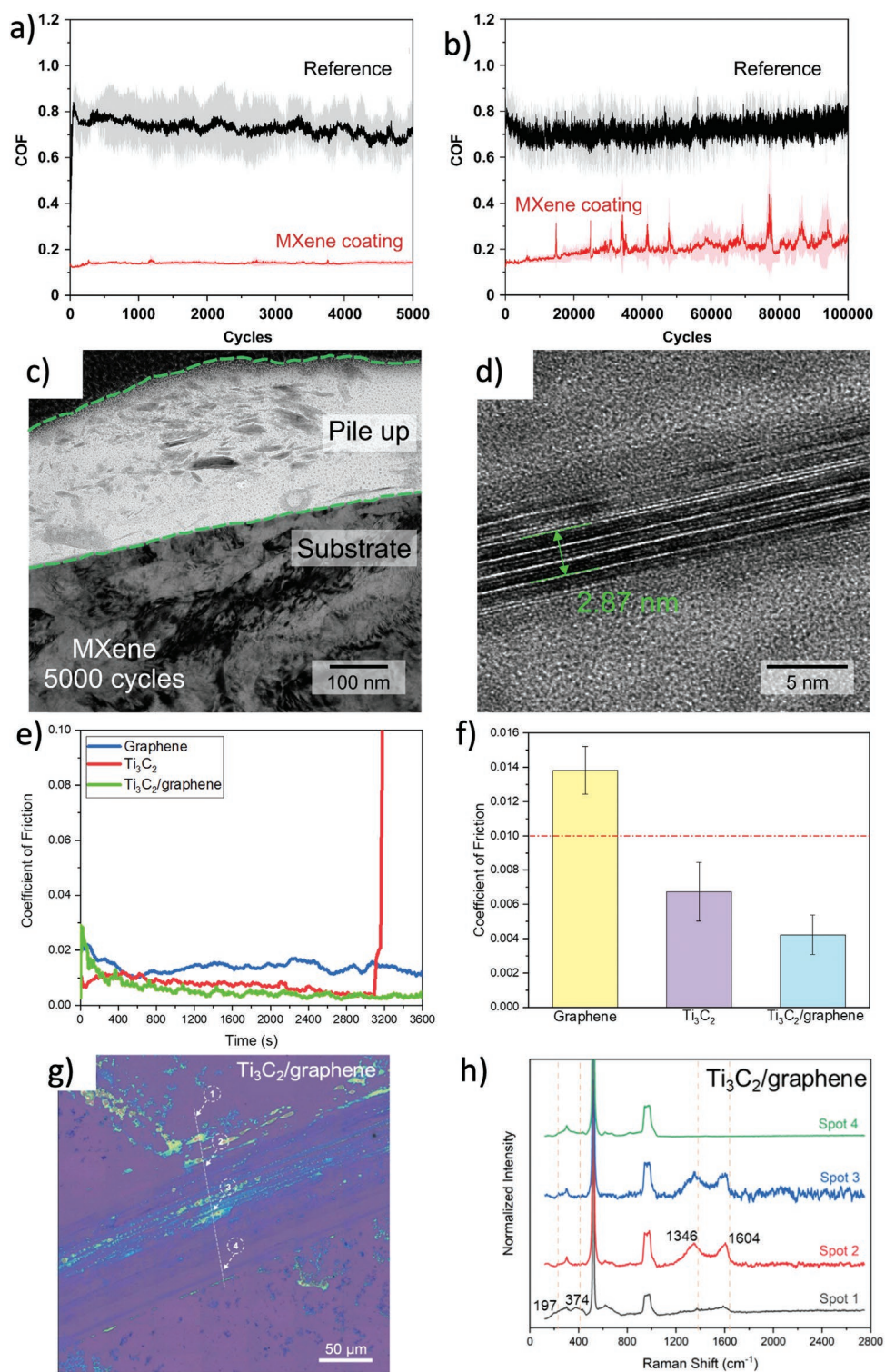


**Figure 4.** MXenes as solid lubricant coatings. a,b) Temporal evolution of the CoF of electrospayed 100 nm-thick ml- $\text{Ti}_3\text{C}_2\text{T}_x$  coatings for 5000 (a) and 100 000 (b) sliding cycles. c,d) TEM images of the formed tribofilms verifying the presence of degraded MXene flakes in the tribofilm, promoting the observed durability and longevity. a–d) Reproduced with permission.<sup>[46]</sup> Copyright 2021, American Chemical Society. e) Evolution and f) comparison of the stable CoFs for spray-coated graphene,  $\text{Ti}_3\text{C}_2\text{T}_x$ , and  $\text{Ti}_3\text{C}_2\text{T}_x$ -graphene nanocomposite coatings, demonstrating macroscale superlubricity of neat  $\text{Ti}_3\text{C}_2\text{T}_x$  and MXene-graphene nanocomposite coatings; g) optical microscopy image of the wear track of the  $\text{Ti}_3\text{C}_2\text{T}_x$ -graphene nanocomposites; and h) Raman spectra from the representative spots within the wear track. e–h) Reproduced with permission.<sup>[51]</sup> Copyright 2021, Elsevier.



**Table 1.** Comparison of the solid lubrication performance of different 2D nanomaterials and nanocomposites. To allow for a fair comparison, studies were subdivided depending on sliding mode (unidirectional and linear-reciprocating sliding). Additionally, a normalized wear life has been calculated by considering the sliding distance divided by the contact pressure and coating thickness.

Solid lubricant coating	Coating thickness [ $\mu\text{m}$ ]	Contact pressure [GPa]	CoF	Sliding distance [m]	Normalized wear life [ $\text{m (GPa } \mu\text{m)}^{-1}$ ]
Unidirectional sliding (rotation)					
Graphene <sup>[87]</sup>	0.01	0.37	0.23	190	51 351
GO <sup>[88]</sup>	0.50	0.70	0.27	35.8	50
MoS <sub>2</sub> <sup>[89]</sup>	1.40	0.30	0.220	3364.6	721
WS <sub>2</sub> <sup>[90]</sup>	1.00	0.96	0.125	386.4	371
WS <sub>2</sub> <sup>[91]</sup>	0.50	0.58	0.075	50.3	58
MoS <sub>2</sub> /WS <sub>2</sub> <sup>[91]</sup>	0.50	0.58	0.075	122.5	142
Ti <sub>3</sub> C <sub>2</sub> T <sub>x</sub> <sup>[80]</sup>	3.00	0.80	0.24	251.2	67
MoS <sub>2</sub> /GO <sup>[85]</sup>	2.5	0.99	0.085	23 000	9293
Linear-reciprocating sliding					
Graphene <sup>[92]</sup>	0.003	0.22	0.20	4	293
GO <sup>[93]</sup>	0.002	0.53	0.125	1	265
MoS <sub>2</sub> <sup>[94]</sup>	1.00	1.03	0.160	16	16
Ti <sub>3</sub> C <sub>2</sub> T <sub>x</sub> <sup>[46]</sup>	0.10	0.30	0.16	120	360
Graphene/MoS <sub>2</sub> <sup>[95]</sup>	4.00	0.50	0.01	1000	125

provide any benchmark for these conditions yet. Moreover, we have normalized the useful wear life considering the total sliding distance, the coating thickness, and the contact pressure to allow for better comparability of the presented studies conducted under different experimental conditions and using variable coating thicknesses (amount of lubricious material in the contact zone). Under unidirectional sliding, graphene and GO/MoS<sub>2</sub> composites show an outstanding normalized wear life of 51 351 and 9293 m (GPa  $\mu\text{m}$ )<sup>-1</sup>, respectively. For linear-reciprocating sliding, MXene coatings demonstrate an excellent wear performance with a normalized wear life of 360 m (GPa  $\mu\text{m}$ )<sup>-1</sup>, outperforming graphene (293 m (GPa  $\mu\text{m}$ )<sup>-1</sup>), GO (265 m (GPa  $\mu\text{m}$ )<sup>-1</sup>), and graphene/MoS<sub>2</sub> composites (125 m (GPa  $\mu\text{m}$ )<sup>-1</sup>). It should be noted that due to the early stage of MXene tribology, we anticipate even better results for MXene solid lubricant coatings in the future, leading to a significantly improved wear life and durability.

The first application of MXene solid lubrication ability and, therefore, a partial knowledge transfer to component test rigs have been verified by Marian et al., who used ml-Ti<sub>3</sub>C<sub>2</sub>T<sub>x</sub> coatings in thrust ball bearings<sup>[96]</sup> and rolling bearings.<sup>[47]</sup> In component-level tests under more realistic working conditions, improved wear resistance with extended wear life based upon the formation of beneficial tribofilms were observed.

## 6. MXenes as Fillers in Composites

Composites reinforced by 2D nanomaterials have gained attention in tribology due to enhanced mechanical properties and superior corrosion resistance, thus reducing friction and extending the resulting wear lifetime.<sup>[97,98]</sup> When designing composites, special attention needs to be paid to the structural and chemical compatibility of the matrix and the selected reinforcement phase. Only for chemically and structurally

compatible constituents can smooth and mechanically strong interfaces be created, which ensure the proper stress transfer from the softer matrix to the stiffer filler, thus enhancing the mechanical properties of the composites.<sup>[55,97–99]</sup> Apart from the overall compatibility, the reinforcement phase should be homogeneously distributed throughout the entire bulk to generate gradient-free composite properties. In this regard, the dispersibility of the nanofillers in the matrix plays a crucial role.<sup>[55,61]</sup> In tribology, a homogeneous filler distribution connects with the potential release of lubricious material to the tribological contact once wear is initiated, which can help to extend the useful wear lifetime of the composite.<sup>[26,55,97]</sup> This aspect becomes particularly interesting for composites reinforced by MXenes, since the released fresh material can ultimately help to form new tribofilms, thus inducing a longer-lasting effect.<sup>[26,55,97]</sup>

With respect to polymeric matrices, ultrahigh-molecular-weight polyethylene (UHMWPE)<sup>[100]</sup> and epoxy<sup>[101,102–107]</sup> have been reinforced by as-synthesized ml-<sup>[100,104,105,107]</sup> or d-MXenes.<sup>[101,102,104,106,108]</sup> The enhanced mechanical properties of the composites (hardness, tensile strength, failure strength, flexural strength, etc.) induced by MXene addition together with their ability to form beneficial tribofilms improved the resulting friction and wear performance.<sup>[26,55,105–107]</sup> Du et al.<sup>[105]</sup> studied epoxy composites with very high filler contents of up to 90 wt% d-Ti<sub>3</sub>C<sub>2</sub>T<sub>x</sub>, and they showed the essential role of the tribofilm formation and its transfer to the tribological counterbody that improved the performance of polymeric composites. Besides the pure MXenes, nanocomposites consisting of 2D MXenes and 0D nanoparticles including Ag,<sup>[104]</sup> Al<sub>2</sub>O<sub>3</sub>,<sup>[109]</sup> TiO<sub>2</sub>,<sup>[110]</sup> and ZrO<sub>2</sub><sup>[110]</sup> have been used to reinforce epoxy, resulting in friction and wear reductions. The beneficial tribological effects observed for 2D/0D nanofillers in epoxy were mainly traced back to the formation of a hybrid tribofilm with good substrate adhesion. Apart from 2D/0D nanocomposites, 2D/2D nanocomposites such as d-Ti<sub>3</sub>C<sub>2</sub>T<sub>x</sub>/graphene have demonstrated



wear rate reduction by up to 90% ascribed to the generation of a self-lubricating film consisting of both nanomaterials.<sup>[102]</sup>

Besides polymer, metallic, and ceramic matrices,<sup>[111]</sup> such as copper,<sup>[112,113]</sup> aluminum,<sup>[114]</sup> and silicate ceramics,<sup>[115]</sup> have been reinforced by ml-<sup>[113–115]</sup> and d-Ti<sub>3</sub>C<sub>2</sub>T<sub>x</sub><sup>[112]</sup> to enhance the resulting friction and wear performance. Initial studies verified that electro-deposited Ti<sub>3</sub>C<sub>2</sub>T<sub>x</sub>/Cu composites resulted in a stable and low CoF as well as reduced wear rate due to the formation of a MXene tribofilm.<sup>[112]</sup> Similar experimental trends were observed in the first tribological study using silicate ceramics reinforced by Ti<sub>3</sub>C<sub>2</sub>T<sub>x</sub>.<sup>[115]</sup>

Much effort has been dedicated to MXene chemical functionalization via their intrinsic surface terminations serving as anchoring points for other molecules to improve MXene dispersibility and phase stability in different matrices. In this regard, it has been demonstrated that chemical functionalization can tailor MXene wettability with polymeric matrices leading to improved compatibility and enhanced interfacial strength<sup>[116,117]</sup> and the formation of covalent bonds.<sup>[118]</sup> Moreover, functionalized Ti<sub>3</sub>C<sub>2</sub>T<sub>x</sub> used as filler material has shown improvements in mechanical properties and corrosion resistance of epoxy and polyurethane matrices.<sup>[117]</sup> With respect to friction and wear, amino-functionalized d-Ti<sub>3</sub>C<sub>2</sub>T<sub>x</sub> improved the dispersibility in and compatibility with epoxy resin (enhanced interfacial strength), which led to decreased friction and wear rates by 35% and 72%, respectively.<sup>[108]</sup> These results were supported by Qu et al., who showed an enhanced interfacial strength for polydopamine/amino silane functionalized Ti<sub>3</sub>C<sub>2</sub>T<sub>x</sub> nanosheets and related improvements in friction and anti-wear performance.<sup>[119]</sup>

## 7. Nanotribology of MXenes

Nanotribological experiments using atomic and friction force microscopy (AFM and FFM)<sup>[34,120–122]</sup> have revealed the potential of ml-,<sup>[120,122]</sup> single-flake Ti<sub>3</sub>C<sub>2</sub>T<sub>x</sub>,<sup>[121]</sup> as well as Nb<sub>2</sub>CT<sub>x</sub><sup>[123]</sup> to reduce friction at the nanoscale (≈40% reduction compared to SiO<sub>2</sub> substrates<sup>[122]</sup>). Friction at the nanoscale depends on the temperature and the relative humidity,<sup>[120,121]</sup> as well as on the MXene synthesis route.<sup>[121]</sup> MXenes prepared by HF and HCl-LiF etching, as well as tetramethylammonium hydroxide delamination, showed notably different pull-off and slide-off forces, frictional hysteresis,<sup>[121]</sup> contact angles, and work of adhesion. These changes were cross-correlated with the surface chemistry/terminations defined by the synthesis route.<sup>[121]</sup> Studying the nanotribology of MXenes with different M verified that ml-Nb<sub>2</sub>CT<sub>x</sub> provided lower adhesion and friction compared to ml-Ti<sub>3</sub>C<sub>2</sub>T<sub>x</sub>, which was explained by differences in the surface dipole moments due to different MXene structures.<sup>[123]</sup> Very recently, Serles et al. experimentally demonstrated that Ti<sub>3</sub>C<sub>2</sub>T<sub>x</sub> does not show the typical layer dependence known for other 2D nanomaterials such as graphene and MoS<sub>2</sub>,<sup>[124]</sup> which was further confirmed by a recent AFM study.<sup>[125]</sup> They verified that the resulting frictional response is mainly governed by the surface chemistry of the materials. Through thermal annealing, the amount of –OH terminations was reduced, thus lowering friction by 57% compared to the untreated, as-received MXene.

Some of us have recently studied friction between MXenes and other 2D materials using AFM.<sup>[34]</sup> For this purpose, Ti<sub>3</sub>C<sub>2</sub>T<sub>x</sub> and Ti<sub>2</sub>CT<sub>x</sub> MXene coated SiO<sub>2</sub> spherical AFM probes were slid against films of 2D materials with varying number of monolayers deposited on the substrate. Over the 15 nm sliding distance, the measured nanoscale CoFs for all the investigated 2D interfaces were below 0.01. However, hydrogen bonding involving –O– and –OH surface terminating groups on MXenes induced higher friction forces for the MXene/MXene contacts compared to other contacts. Moreover, a less significant number-of-monolayers effect on the friction was observed for MXenes due to their thicker monolayers (3 atomic layers or more) compared with other 2D materials. Overall, more studies in this area are needed to further our understanding of the mechanisms of MXene friction and fully unlock the potential of MXenes as tunable lubricants at the nanoscale.

## 8. Computational Modeling of MXene Tribology

Computational modeling has proven to be instrumental in developing the tribological applications of nearly all existing 2D materials. However, only a few computational studies on MXene tribology have been performed up to now, mainly focusing on the interflake adhesion and sliding of titanium carbide MXenes. The binding energies of Ti<sub>3</sub>C<sub>2</sub>T<sub>2</sub> (T = –OH, –O–, or –F) were calculated using density functional theory (DFT) with semiempirical van der Waals corrections.<sup>[32]</sup> The results indicated that these surface terminations weaken the interlayer adhesion compared to the bare layers, and the coupling strongly depends on the terminating species. The same approach applied to study the effects of M in M<sub>2</sub>CO<sub>2</sub> MXene bilayers (M = Ti, Zr, Nb, Mo, Hf, Ta, and W) revealed increased sliding energy barriers with a larger in-plane lattice constant. Additionally, it was observed that normal and in-plane biaxial strain in Ti<sub>2</sub>CO<sub>2</sub> increased its resistance to sliding, while in-plane uniaxial tension decreased the sliding energy barrier due to the anisotropic expansion of the surface.<sup>[126]</sup>

A combined DFT and ReaxFF molecular dynamics (MD) study yielded a CoF of 0.27 for Ti<sub>3</sub>C<sub>2</sub>O<sub>2</sub> for applied loads of less than 1.2 GPa.<sup>[127]</sup> The CoF was higher in the presence of metal and terminal atom vacancies, while –OH and –OCH<sub>3</sub> terminations reduced it. These studies highlight the role of T and M in the adhesion and shear strength of MXenes. A systematic analysis of these and other intrinsic MXene characteristics in tribology is still lacking. As suggested in **Figure 5a**, a computational high-throughput screening<sup>[128]</sup> of the interlayer interactions and their modification under load can be envisaged to select the most suitable MXene composition and terminations for a specific (nano)tribological application.<sup>[129]</sup> The high-throughput screening of relevant properties at solid interfaces performed for other materials<sup>[130]</sup> revealed, for example, the relationship between the adhesion and shear strength<sup>[131]</sup> and the connections between the interfacial electronic and tribological properties.<sup>[132]</sup> Because of the large variability in composition, monolayer thickness (1 ≤ n ≤ 4), surface chemistry, as well as relative orientation and load-carrying capacity on the facing layers, the computational screening of MXene tribological performance will greatly benefit from

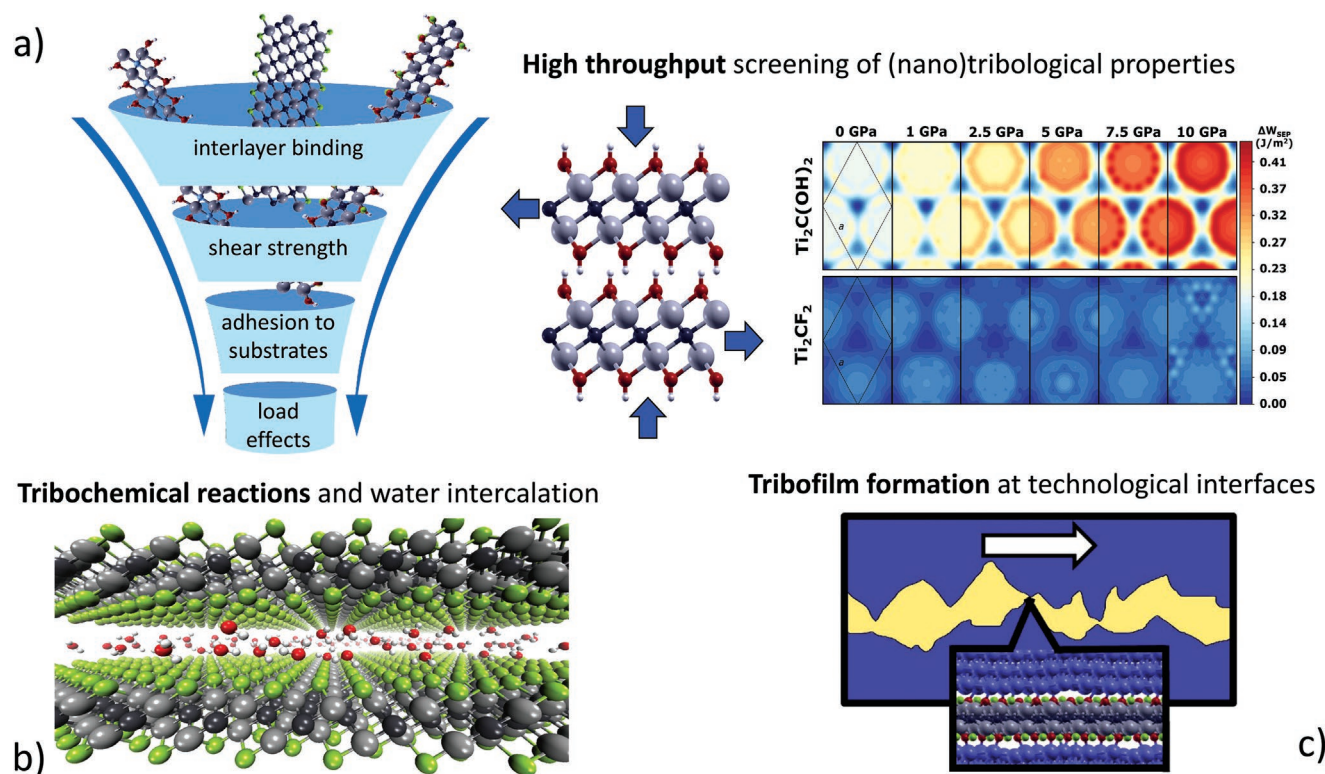


**Figure 5.** a–c) Proposed computational methodologies to elucidate physical–chemical properties (a) and atomistic mechanisms (b,c) relevant for the MXene tribological performance.

machine-learning algorithms. The Bayesian analysis and transfer learning models have been recently shown to correctly predict the maximum energy barrier at the onset of interlayer sliding in 2D materials.<sup>[133]</sup>

In addition to static first-principles calculations, modeling of the sliding dynamics is essential to describe the effects of energy dissipation through phonons and other collective mechanisms that are activated in non-equilibrium conditions. The effect of intercalated moieties can be also explored, similar to studies considering the effect of water in the tribochemistry of graphene and MoS<sub>2</sub>.<sup>[134]</sup> This is particularly relevant for MXenes, which, on the one hand, almost always contain intercalated or adsorbed H<sub>2</sub>O molecules (Figure 5b), and on the other hand, are prone to hydrolysis.<sup>[43,44]</sup> The passivation effect, recently observed for Ti<sub>3</sub>C<sub>2</sub>-graphene nanocomposites thus extending the superlubricity and wear life of MXenes,<sup>[51]</sup> is also interesting and worth exploring through further simulation efforts aimed at probing the mechanisms in more detail.

The reduced size along one dimension renders 2D materials more amenable to ab initio MD, which is necessary for capturing the activation mechanisms, quantum mechanical in nature, of tribochemical reactions. The observation of a superior wear resistance of Ti<sub>3</sub>C<sub>2</sub>T<sub>x</sub> due to the tribofilm formation<sup>[46]</sup> necessitates the detailed exploration of MXene mechanochemistry at the microasperity level involving contacts of steel or other technologically relevant materials, as schematically illustrated in Figure 5c. Multiscale dynamic simulations represent a powerful tool for modeling over relevant time and size scales that are out of reach of ab initio MD, while still preserving an accurate description of the underlying chemical processes. In

the past, a hybrid quantum mechanics/molecular mechanics (QM/MM) scheme has been used for real-time monitoring of the early stages of tribofilm formation from additives to engine oils.<sup>[135]</sup> In future efforts, the recently developed machine-learning-based force fields may be also used for performing MD simulations with the accuracy of QM and at the speed typical for MM calculations. These accurate and fast MD simulations will permit monitoring tribochemical reactions that lead to the tribofilm formation on the time (length) scales of nanoseconds (nanometers). For instance, we envision simulating a MXene flake rubbed within two surfaces, for example, of iron or iron oxide, and monitor the potential decomposition of the flake and atomic intermixing. By recording the evolution of the frictional force during the simulation, information about the mechanisms of the tribofilm formation and its effect on sliding could be gained. A similar analysis could be performed in the presence of environmental molecules such as water molecules to elucidate the effect of moisture on MXenes' lubricity. The assessment of the thermodynamic driving forces for the observed reactions, which becomes possible through energy calculations in static conditions, will enable deriving general conclusions on the system behavior under different environmental conditions.

Moreover, we want to emphasize the potential of popular artificial intelligence and machine learning methodologies for future understanding of MXene tribology. Often the relationship between the structure/composition and function of a lubricant turns out to be challenging to capture and even harder to predict, since it results from the interplay of concurrent physical phenomena at multiple scales. Historically, the design of

lubricants has often relied on human intuition to interpret and deduce that relationship. In this context, MXene overall tunability in terms of chemical composition, surface terminations, thickness, and functionalization creates an overwhelming space for design and further improvement. Therefore, the use of machine learning approaches such as deep learning or generative methods could be particularly beneficial. These methods can capture general trends in very large datasets populated by real world or in silico experimental results, thus predicting the lubricating properties of novel or improved compounds (two recent perspectives on the use of artificial intelligence in tribology can be found in refs. [136,137]).

## 9. Summary and Perspective Outlook

The research area of MXene tribology is still in its infancy but has already demonstrated the potential of these 2D materials to reduce friction and wear when used as lubricant additives, filler materials in composites, or solid lubricant coatings in combination with other 2D materials or nanoparticles. Based upon the summarized state-of-the-art, we identify the missing puzzle pieces and bottlenecks as well as give specific recommendations to explore the full tribological potential of MXenes in the following sub-sections.

### 9.1. Tribofilm Formation

Irrespective of MXene usage as additive, filler, or solid lubricant coating, their beneficial effects on friction and wear are commonly traced back to the tribofilm formation and transfer to the rubbing counterbody, although more detailed characterization with in situ and ex situ characterization techniques would be valuable to gain insight into the mechanism of formation of such tribofilms. In this regard, only initial experiments have been realized, while the complete system approach to fully explore the tribological potential of MXenes is still missing. More work needs to be dedicated to elucidating the underlying mechanisms of friction and wear reduction, since little is known about the tribofilm morphology, chemistry, mechanical properties, and formation mechanisms, necessitating more experimental and theoretical insights. Regarding the morphology and chemistry of the formed tribofilms, we suggest characterizing them by complementary high-resolution characterization techniques combining spatially resolved X-ray photoelectron spectroscopy, high-resolution transmission electron spectroscopy, electron energy loss spectroscopy, and synchrotron techniques. We anticipate that AFM methods such as recording force-distance curves or using the amplitude modulation/frequency modulation mode can shed additional light on the elastic mechanical properties of the considerably thin tribofilms. Related to the underlying formation mechanism, we recommend performing cycle-dependent running-in experiments using different substrate and counterbody materials as well as variable tribological testing conditions (relative humidity, contact pressure, etc.) and environmental conditions. The time-dependent characteristics of the tribofilms (chemistry, structure, morphology, adhesion, among others) formed

on both rubbing surfaces should be holistically characterized using the aforementioned high-resolution techniques to cross-correlate MXene overall reactivity with used materials, experimental conditions, and the resulting temporal CoF evolution. These newly gained experimental insights need to be verified and further understood by well-designed numerical DFT and MD modeling. In this regard, we anticipate that machine learning can help to find cross-correlations between MXene tribological performance, materials characterization data, and the operational parameters, thus further establishing kinematic and load conditions for tribofilm formation and transfer. High-throughput modeling techniques may help us find beneficial material combinations, reduce trial-and-error testing, and boost the entire field of hybrid nanocomposites for liquid and solid lubrication (including filler materials) as developed approaches can be transferred to other materials beyond MXenes.

### 9.2. Lubricant Additives

The use of MXenes as lubricant additives is still challenging and greatly depends on their compatibility with and dispersibility in the liquid phase. MXenes are strongly hydrophilic, while most liquid lubricants are hydrophobic (oils and greases), and water is reactive. Solutions to both the compatibility and chemical stability problems will greatly benefit from better knowledge and understanding of MXenes chemistry. In this regard, enhanced synthetic approaches to tailor the resulting surface terminations and strategies to chemically modify their surface or the design of heterostructures are considered as effective ways to manipulate MXenes' compatibility with liquid media. More emphasis needs to be put on the detailed analysis of MXene dispersion stability, especially in operando lubrication conditions (elevated temperatures, long times, and effects of the environment). Experimentally measured properties, such as zeta potential, particle size, and sedimentation speed, should guide the optimal formulation of liquid lubricants with MXenes. Based on the existing literature, the effect of different MXene concentrations in non-polar lubricants on the resulting rheological properties such as viscosity and shear thinning, among others, is nearly unexplored. We recommend combining concentration-dependent viscosity measurements with tribological tests using more sophisticated test rigs with the possibility to adjust temperature, load, and slide-to-roll ratio. Following this procedure, the tribological performance of MXenes under lubricated conditions can be studied depending on the acting oil film thickness under different lubrication regimes (boundary, mixed, electrohydrodynamic, and full film lubrication) and correlated with the contact severity. Once the knowledge for non-additivated base oils has been sufficiently gained, we suggest studying MXenes as additives in formulated oils containing commercial additive complexes, thus studying their interaction with other extreme-pressure or anti-wear additives. Besides non-polar lubricants, more research should be dedicated to the use of MXenes in green (polar) lubricants such as water, ethanol, glycerol, among others, due to their inherent hydrophilicity. We envision that the successful application of MXenes in these green lubricants could pave the way toward accelerated decarbonization and reduced CO<sub>2</sub> emissions.



### 9.3. Solid Lubricant Coatings

Although initial studies have demonstrated very promising results for MXene solid lubricant coatings, more systematic research as a function of the coating thickness and tribological testing parameters with particular emphasis on contact pressure, relative humidity, environmental conditions, and material pairing, among others, need to be conducted. Most of the published studies used coatings made of ml-MXenes produced by simple deposition techniques resulting in coatings with imperfect adhesion and homogeneity. In this regard, more emphasis needs to be put on the fabrication of uniform and homogeneous coatings with good coating-substrate adhesion and adjustable coating thickness. Advanced deposition techniques (e.g., electrophoretic deposition) and complete delamination, as well as the chemical functionalization of MXenes, can improve their adhesive and interfacial properties, thus boosting their tribological response under solid lubrication. Moreover, MXene adhesion to different bulk<sup>[50]</sup> and 2D materials,<sup>[35]</sup> which itself is another interesting emerging topic, bears clear implications for MXene tribology and needs to be further studied by experimental and computational techniques.

The tribological performance under dry conditions can be notably improved by the combined use of surface textures and solid lubricants,<sup>[8]</sup> which is also a promising avenue to be explored for MXenes.<sup>[138]</sup> Initial studies combining grooves<sup>[139]</sup> or bionic cross-like textures<sup>[140]</sup> and MXenes (ml-Ti<sub>3</sub>C<sub>2</sub>T<sub>x</sub><sup>[139]</sup> and NbC<sub>2</sub>T<sub>x</sub><sup>[140]</sup>) have shown beneficial effects with potential for further improvements. However, the studied systems are rather complex and difficult to analyze due to the usage of MXenes, surface textures, and self-lubricating Sn–Ag–Cu alloys. Therefore, we suggest the use of simplified models to start with, for example, combining MXenes with hemispherical textures, which bear the possibility of storing the solid lubricant. In this regard, special attention needs to be paid to the deposition of MXenes onto the textured surfaces. We anticipate that more fundamental knowledge about potential synergistic effects can be gained by less complex material pairing and simpler surface textures. Besides surface textures, the use of composite coatings combining MXenes with other 0D or 2D nanomaterials seems to be a promising strategy to further improve the friction and wear response under solid lubrication. In this context, the additional nanomaterial can help to prevent MXene restacking and agglomeration, which is essential to guarantee the proper formation of beneficial tribofilms. Additionally, the combined use of different nanomaterials with complementary tribological characteristics, such as MXenes with graphene, GO, or TMDCs, is expected to induce synergistic effects, thus simultaneously enhancing friction and wear. These composite coatings can be deposited with different coating morphologies such as random mixes or layer-by-layer coatings, which opens even more paths to further manipulate and optimize the resulting friction and wear performance.

### 9.4. Fillers in Composites

While more studies focused on MXene in polymeric matrices to improve mechanical and tribological properties, less attention

has been given to metallic and ceramic matrices. The compatibility and wettability of MXenes with the respective matrices and the effects of MXene concentrations need to be elucidated in detail. High-resolution characterizations of the filler–matrix interfaces are crucial to understand the involved interfacial reactions, thus ensuring a proper stress transfer. Weak interfaces can lead to the creation of defects and potential for crack initiation. Controlled surface functionalization is needed for the design of proper interfacial reactions to improve the interfacial interactions. Further studies are needed to better understand MXenes' chemical and structural changes due to temperatures and mechanical stresses, which may directly affect MXenes' ability to form beneficial tribofilms. Lastly, a homogeneous distribution of the filler material throughout the entire composite body is essential to induce long-lasting tribological effects. However, experimental ways to improve the respective filler distribution are yet to be explored.

### 9.5. Tribological Applications

Besides simplified ball-on-disk tribometry, initial studies using ml-Ti<sub>3</sub>C<sub>2</sub>T<sub>x</sub> in component-level test rigs (thrust ball and rolling bearings) show promising results in dry-running mechanical systems, thus verifying the wear resistance of MXenes in advanced tribosystems under more realistic testing conditions. Inspired by these initial results, more effort should be dedicated toward the exploration of MXene performance in wear-critical components using component- and system-level test rigs to fully reveal their tribological potential and to allow for a knowledge transfer to real machine components. This aspect holds true for MXene solid lubrication coatings, but also applies equally to their usage as lubricant additives (oils and greases) when ensuring sufficiently long dispersion stability.

Notably, the newly emerged area of MXene tribology will probably have implications beyond classical tribology or lubrication. In this regard, just one example out of many the reader may think about: MXene-based nano-triboelectric generators.<sup>[141]</sup> For this application, further progress in our understanding of the mechanisms and factors influencing MXene conductivity (briefly touched upon above), chemical stability, and adhesion will be essential. Moreover, nano-triboelectric generators are prone to wear-off over time, which diminishes the resulting output voltage and deteriorates the respective surface topography. We hypothesize that the excellent wear resistance of MXenes could be beneficial to protect the respective surfaces, while ensuring excellent electric properties at the same time. Due to the reported antibacterial and antiviral properties of MXenes, another prospective area of their applications is biotribology. Regarding implant materials (mainly Ti-based or polymer composites), new strategies are sought to improve their wear resistance and avoid generation of debris known to trigger tissue inflammation. The excellent wear resistance of Ti<sub>3</sub>C<sub>2</sub>T<sub>x</sub> could enhance the design of new implant materials. Besides implants, similar effects of MXenes will be beneficial in materials for endoscopes and other devices for minimally invasive surgery, as well as cardiovascular devices and dental implants.

## 9.6. MXenes' Chemical Stability and Interaction with the Environment

Only a handful of MXenes (mostly  $Ti_3C_2T_x$  and  $Nb_2CT_x$ ) have been investigated in tribological applications so far, and the performance of other MXenes, as well as the potential of tribology-tailored design of MXenes, remain to be explored. MXenes provide an unmatched tunability of composition, monolayer thickness, and surface chemistry, which still need to be leveraged for tribological applications. Combining MXenes with other 2D materials is also a promising avenue, as evidenced by the first measurements on  $Ti_3C_2T_x$ -graphene composite films.<sup>[51]</sup> These combinations can be aimed at further reducing friction and wear compared to neat MXenes or graphene, as well as protecting MXenes from chemical interactions with the environment, provided we better understand these chemical interactions.

## Acknowledgements

All the authors contributed equally to this work. A.R. gratefully acknowledges the financial support provided by ANID within the project, Fondecyt Regular 1220331 and Fondecyt EQM190057. A.S. acknowledges that part of this work was performed at the Center for Nanoscale Materials, a U.S. Department of Energy Office of Science User Facility, and supported by the U.S. Department of Energy, Office of Science, under Contract No. DE-AC02-06CH11357. M.C.R. acknowledges the SLIDE project that has received funding from the European Research Council (ERC) under the European Union's Horizon 2020 research and innovation programme (Grant Agreement No. 865633). B.A. thanks the Office Naval Research (ONR) for partially funding this research under award number N00014-21-1-2799. V.N.M. gratefully acknowledges partial financial support of this work by the National Science Foundation through Grant no. CMMI-1930881 and the National Eye Institute of the National Institutes of Health under Award Number 1R15EY029813-01A1.

## Conflict of Interest

The authors declare no conflict of interest.

## Keywords

2D materials, 2D transition metal carbides, 2D transition metal nitrides, friction, mechanical properties, MXenes

Received: August 24, 2022

Revised: October 6, 2022

Published online: December 20, 2022

- [1] a) K. Holmberg, A. Erdemir, *Tribol. Int.* **2019**, *135*, 389; b) M. Woydt, T. Gradt, T. Hosenfeldt, R. Luther, A. Rienäcker, F.-J. Wetzlar, C. Wincierz, *Tribologie in Deutschland-Querschnittstechnologie zur Minderung von CO<sub>2</sub>-Emissionen und zur Ressourcenschonung*, Gesellschaft für Tribologie eV, Jülich, Germany **2019**, p. 33; c) E. Ciulli, *Front. Mech. Eng.* **2019**, *5*, 55.
- [2] a) A. Sarkar, E. M. Krop, *Curr. Opin. Food Sci.* **2019**, *27*, 64; b) W. Xu, S. Yu, M. Zhong, *Friction* **2022**, *10*, 1927; c) A. Rosenkranz,

- M. Marian, R. Shah, B. Gashi, S. Zhang, E. Bordeu, N. Brossard, *Adv. Colloid Interface Sci.* **2021**, *296*, 102520; d) L. Laguna, A. Sarkar, *Tribol.-Mater., Surf. Interfaces* **2017**, *11*, 116.
- [3] a) H. Pult, S. G. P. Tosatti, N. D. Spencer, J.-M. Asfour, M. Ebenhoch, P. J. Murphy, *Ocul. Surf.* **2015**, *13*, 236; b) O. Sterner, R. Aeschlimann, S. Zürcher, C. Scales, D. Riederer, N. D. Spencer, S. G. P. Tosatti, *Tribol. Lett.* **2016**, *63*, 9; c) S. Derler, L. C. Gerhardt, *Tribol. Lett.* **2012**, *45*, 1.
- [4] R. I. Taylor, *Lubricants* **2021**, *9*, 66.
- [5] M. Woydt, *Wear* **2022**, *488*, 204134.
- [6] R. Stribeck, *Die Wesentlichen Eigenschaften der Gleit- und Rollenlager*, Julius Springer, Berlin, Germany **1903**.
- [7] T. W. Scharf, S. V. Prasad, *J. Mater. Sci.* **2013**, *48*, 511.
- [8] A. Rosenkranz, H. L. Costa, M. Z. Baykara, A. Martini, *Tribol. Int.* **2021**, *155*, 106792.
- [9] I. Minami, *Appl. Sci.* **2017**, *7*, 445.
- [10] J. Zhao, Y. Huang, Y. He, Y. Shi, *Friction* **2021**, *9*, 891.
- [11] H. Xiao, S. Liu, *Mater. Des.* **2017**, *135*, 319.
- [12] a) A. H. Castro Neto, F. Guinea, N. M. R. Peres, K. S. Novoselov, A. K. Geim, *Rev. Mod. Phys.* **2009**, *81*, 109; b) A. K. Geim, K. S. Novoselov, in *Nanoscience and Technology*, Macmillan Publishers Ltd, London, UK, **2009**, p. 11; c) A. K. Geim, *Science* **2009**, *324*, 1530.
- [13] Y. Guo, X. Zhou, K. Lee, H. C. Yoon, Q. Xu, D. Wang, *Nanotechnology* **2021**, *32*, 312002.
- [14] a) A. Rosenkranz, Y. Liu, L. Yang, L. Chen, *Appl. Nanosci.* **2020**, *10*, 3353; b) L. Liu, M. Zhou, L. Jin, L. Li, Y. Mo, G. Su, X. Li, H. Zhu, Y. Tian, *Friction* **2019**, *7*, 199.
- [15] S. Zhang, T. Ma, A. Erdemir, Q. Li, *Mater. Today* **2019**, *26*, 67.
- [16] A. VahidMohammadi, J. Rosen, Y. Gogotsi, *Science* **2021**, *372*, eabf1581.
- [17] W. Hong, B. C. Wyatt, S. K. Nemani, B. Anasori, *MRS Bull.* **2020**, *45*, 850.
- [18] O. Mashtalir, M. Naguib, V. N. Mochalin, Y. Dall'Agnese, M. Heon, M. W. Barsoum, Y. Gogotsi, *Nat. Commun.* **2013**, *4*, 1716.
- [19] M. Sokol, V. N. Natu, S. Kota, M. W. Barsoum, *Trends Chem.* **2019**, *1*, 210.
- [20] a) M. Naguib, M. Kurtoglu, V. Presser, J. Lu, J. Niu, M. Heon, L. Hultman, Y. Gogotsi, M. W. Barsoum, *Adv. Mater.* **2011**, *23*, 4248; b) M. Alhabeab, K. Maleski, B. Anasori, P. Lelyukh, L. Clark, S. Sin, Y. Gogotsi, *Chem. Mater.* **2017**, *29*, 7633.
- [21] M. Ghidui, M. R. Lukatskaya, M. Q. Zhao, Y. Gogotsi, M. B. Barsoum, *Nature* **2014**, *516*, 78.
- [22] Y. Li, H. Shao, Z. Lin, J. Lu, L. Liu, B. Duployer, P. O. A. Persson, P. Eklund, L. Hultman, M. Li, K. Chen, X. H. Zha, S. Du, P. Rozier, Z. Chai, E. Raymundo-Pinero, P. L. Taberna, P. Simon, Q. Huang, *Nat. Mater.* **2020**, *19*, 894.
- [23] V. Kamysbayev, A. S. Filatov, H. Hu, X. Rui, F. Lagunas, D. Wang, R. F. Klie, D. V. Talapin, *Science* **2020**, *369*, 979.
- [24] M. A. Hope, A. C. Forse, K. J. Griffith, M. R. Lukatskaya, M. Ghidui, Y. Gogotsi, C. P. Grey, *Phys. Chem. Chem. Phys.* **2016**, *18*, 5099.
- [25] a) M. Han, K. Maleski, C. E. Shuck, Y. Yang, J. T. Glazar, A. C. Foucher, K. Hantanasirisakul, A. Sarycheva, N. C. Frey, S. J. May, V. B. Shenoy, E. A. Stach, Y. Gogotsi, *J. Am. Chem. Soc.* **2020**, *142*, 19110; b) M. Han, C. E. Shuck, R. Rakhmanov, D. Parchment, B. Anasori, C. M. Koo, G. Friedman, Y. Gogotsi, *ACS Nano* **2020**, *14*, 5008.
- [26] B. C. Wyatt, A. Rosenkranz, B. Anasori, *Adv. Mater.* **2021**, *33*, 2007973.
- [27] a) A. Lipatov, M. Alhabeab, H. Lu, S. Zhao, M. J. Loes, N. S. Vorobeve, Y. Dall'Agnese, Y. Gao, A. Gruverman, Y. Gogotsi, *Adv. Electron. Mater.* **2020**, *6*, 1901382; b) A. Lipatov, H. Lu, M. Alhabeab, B. Anasori, A. Gruverman, Y. Gogotsi, A. Sinititskii, *Sci. Adv.* **2018**, *4*, eaat0491.

- [28] V. N. Borysiuk, V. N. Mochalin, Y. Gogotsi, *Comput. Mater. Sci.* **2018**, *143*, 418.
- [29] T. S. Mathis, K. Maleski, A. Goad, A. Sarycheva, M. Anayee, A. C. Foucher, K. Hantanasirisakul, C. E. Shuck, E. A. Stach, Y. Gogotsi, *ACS Nano* **2021**, *15*, 6420.
- [30] K. Maleski, V. N. Mochalin, Y. Gogotsi, *Chem. Mater.* **2017**, *29*, 1632.
- [31] a) M. R. Lukatskaya, O. Mashtalir, C. E. Ren, Y. Dall'Agnese, P. Rozier, P. L. Taberna, M. Naguib, P. Simon, M. W. Barsoum, Y. Gogotsi, *Science* **2013**, *341*, 1502; b) M. Ghidui, S. Kota, J. Halim, A. W. Sherwood, N. Nedfors, J. Rosen, V. N. Mochalin, M. W. Barsoum, *Chem. Mater.* **2017**, *29*, 1099.
- [32] T. Hu, M. Hu, Z. Li, H. Zhang, C. Zhang, J. Wang, X. Wang, *Phys. Chem. Chem. Phys.* **2016**, *18*, 20256.
- [33] M. Naguib, R. R. Unocic, B. L. Armstrong, J. Nanda, *Dalton Trans.* **2015**, *44*, 9353.
- [34] Y. Li, S. Huang, C. Wei, D. Zhou, B. Li, V. N. Mochalin, C. Wu, *Carbon* **2022**, *196*, 774.
- [35] Y. Li, S. Huang, C. Wei, D. Zhou, B. Li, C. Wu, V. N. Mochalin, *ACS Appl. Mater. Interfaces* **2021**, *13*, 4682.
- [36] A. I. Kharlamov, *Teor. Ehksp. Khim.* **1981**, *17*, 515.
- [37] A. Champagne, J.-C. Charlier, *J. Phys. Mater.* **2020**, *3*, 032006.
- [38] S.-Y. Pang, Y.-T. Wong, S. Yuan, Y. Liu, M.-K. Tsang, Z. Yang, H. Huang, W.-T. Wong, J. Hao, *J. Am. Chem. Soc.* **2019**, *141*, 9610.
- [39] T. Li, L. Yao, Q. Liu, J. Gu, R. Luo, J. Li, X. Yan, W. Wang, P. Liu, B. Chen, W. Zhang, W. Abbas, R. Naz, D. Zhang, *Angew. Chem., Int. Ed.* **2018**, *57*, 6115.
- [40] M. Li, J. Lu, K. Luo, Y. Li, K. Chang, K. Chen, J. Zhou, J. Rosen, L. Hultman, P. Eklund, P. O. Å. Persson, S. Du, Z. Chai, Z. Huang, Q. Huang, *J. Am. Chem. Soc.* **2019**, *141*, 4730.
- [41] A. Jawaid, A. Hassan, G. Neher, D. Nepal, R. Pachter, W. J. Kennedy, S. Ramakrishnan, R. A. Vaia, *ACS Nano* **2021**, *15*, 2771.
- [42] H. Chen, H. Ma, C. Li, *ACS Nano* **2021**, *15*, 15502.
- [43] a) S. Huang, V. N. Mochalin, *Inorg. Chem.* **2019**, *58*, 1958; b) S. Huang, V. N. Mochalin, *ACS Nano* **2020**, *14*, 10251.
- [44] S. Huang, V. N. Mochalin, *Inorg. Chem.* **2022**, *61*, 9877.
- [45] A. Avgustinik, G. Drozdetskaya, S. Ordan'yan, *Powder Metall. Met. Ceram.* **1967**, *6*, 470.
- [46] P. G. Grutzmacher, S. Suarez, A. Tolosa, C. Gachot, G. Song, B. Wang, V. Presser, F. Mücklich, B. Anasori, A. Rosenkranz, *ACS Nano* **2021**, *15*, 8216.
- [47] M. Marian, K. Feile, B. Rothhammer, M. Bartz, S. Wartzack, A. Seynstaal, S. Tressel, S. Krauß, B. Merle, T. Böhm, B. Wang, B. C. Wyatt, B. Anasori, A. Rosenkranz, *Appl. Mater. Today* **2021**, *25*, 101202.
- [48] W. H. Bragg, *An Introduction to Crystal Analysis*, Bell, London, UK **1928**.
- [49] a) A. P. Green, F. P. Bowden, *Proc. R. Soc. London, Ser. A* **1955**, *228*, 191; b) F. P. Bowden, D. Tabor, *Nature* **1942**, *150*, 197.
- [50] Y. Li, S. Huang, C. Wei, C. Wu, V. N. Mochalin, *Nat. Commun.* **2019**, *10*, 3014.
- [51] S. Huang, K. C. Mutyala, A. V. Sumant, V. N. Mochalin, *Mater. Today Adv.* **2021**, *9*, 100133.
- [52] a) R. H. Savage, *J. Appl. Phys.* **1948**, *19*, 1; b) Y. Liu, X. Ge, J. Li, *Appl. Mater. Today* **2020**, *20*, 100662.
- [53] M. Marian, D. Berman, A. Rota, R. L. Jackson, A. Rosenkranz, *Adv. Mater. Interfaces* **2022**, *9*, 2101622.
- [54] D. Berman, A. Erdemir, A. V. Sumant, *ACS Nano* **2018**, *12*, 2122.
- [55] M. Malaki, R. S. Varma, *Adv. Mater.* **2020**, *32*, 2003154.
- [56] X. Yin, J. Jin, X. C. Chen, A. Rosenkranz, J. B. Luo, *ACS Appl. Mater. Interfaces* **2019**, *11*, 32569.
- [57] M. Seredych, C. E. Shuck, D. Pinto, M. Alhabeab, E. Precetti, G. Deysheer, B. Anasori, N. Kurra, Y. Gogotsi, *Chem. Mater.* **2019**, *31*, 3324.
- [58] B. C. Wyatt, S. K. Nemani, K. Desai, H. Kaur, B. Zhang, B. Anasori, *J. Phys. Condens. Matter* **2021**, *33*, 224002.
- [59] X. Miao, S. Liu, L. Ma, Y. Yang, J. Zhu, Z. Li, J. Wang, *Tribol. Int.* **2022**, *167*, 107361.
- [60] W. Zhai, N. Srikanth, L. B. Kong, K. Zhou, *Carbon* **2017**, *119*, 150.
- [61] J. C. Spear, B. W. Ewers, J. D. Batteas, *Nano Today* **2015**, *10*, 301.
- [62] X. Zhang, M. Xue, X. Yang, Z. Wang, G. Luo, Z. Huang, X. Sui, C. Li, *RSC Adv.* **2015**, *5*, 2762.
- [63] Y. Liu, X. Zhang, S. Dong, Z. Ye, Y. Wei, *J. Mater. Sci.* **2016**, *52*, 2200.
- [64] J. Yang, B. Chen, H. Song, H. Tang, C. Li, *Cryst. Res. Technol.* **2014**, *49*, 926.
- [65] Q. Feng, F. Deng, K. Li, M. Dou, S. Zou, F. Huang, *Colloids Surf. A* **2021**, *625*, 126903.
- [66] X. S. F. X. Zhang, G. G. Tang, J. Xu, *Chalcogenide Lett.* **2021**, *18*, 225.
- [67] X. Zhang, Y. Guo, Y. Li, Y. Liu, S. Dong, *Chin. Chem. Lett.* **2019**, *30*, 502.
- [68] M. Xue, Z. Wang, F. Yuan, X. Zhang, W. Wei, H. Tang, C. Li, *RSC Adv.* **2017**, *7*, 4312.
- [69] S. Yi, J. Li, Y. Liu, X. Ge, J. Zhang, J. Luo, *Tribol. Int.* **2021**, *154*, 106695.
- [70] Z. Bao, N. Bing, X. Zhu, H. Xie, W. Yu, *Chem. Eng. J.* **2021**, *406*, 126390.
- [71] H. T. Nguyen, K. H. Chung, *Materials* **2020**, *13*, 5545.
- [72] J. Chen, W. Zhao, *Tribol. Int.* **2021**, *153*, 106598.
- [73] H. Cheng, W. Zhao, *Friction* **2021**, *10*, 398.
- [74] S. Yi, Y. Guo, J. Li, Y. Zhang, A. Zhou, J. Luo, *Friction* **2023**, *11*, 369.
- [75] C. Zhou, Z. Li, S. Liu, L. Ma, T. Zhan, J. Wang, *Tribol. Lett.* **2022**, *70*, 63.
- [76] J. Gao, C.-F. Du, T. Zhang, X. Zhang, Q. Ye, S. Liu, W. Liu, *ACS Appl. Nano Mater.* **2021**, *4*, 11080.
- [77] J. Guo, P. Wu, C. Zeng, W. Wu, X. Zhao, G. Liu, F. Zhou, W. Liu, *Tribol. Int.* **2022**, *170*, 107500.
- [78] P. Feng, Y. Ren, Y. Li, J. He, Z. Zhao, X. Ma, X. Fan, M. Zhu, *Friction* **2022**, *10*, 2018.
- [79] W. Lian, Y. Mai, C. Liu, L. Zhang, S. Li, X. Jie, *Ceram. Int.* **2018**, *44*, 20154.
- [80] M. Marian, G. C. Song, B. Wang, V. M. Fuenzalida, S. Krauß, B. Merle, S. Tressel, S. Wartzack, J. Yu, A. Rosenkranz, *Appl. Surf. Sci.* **2020**, *531*, 147311.
- [81] A. Rosenkranz, P. G. Grützmacher, R. Espinoza, V. M. Fuenzalida, E. Blanco, N. Escalona, F. J. Gracia, R. Villarroel, L. Guo, R. Kang, F. Mücklich, S. Suarez, Z. Zhang, *Appl. Surf. Sci.* **2019**, *494*, 13.
- [82] J. Y. A. Hurtado, P. G. Grützmacher, J. M. Henríquez, D. Zambrano, B. Wang, A. Rosenkranz, *Adv. Eng. Mater.* **2022**, *24*, 2200755.
- [83] X. Yin, J. Jin, X. Chen, A. Rosenkranz, J. Luo, *Adv. Eng. Mater.* **2020**, *22*, 1901369.
- [84] K. C. Mutyala, Y. A. Wu, A. Erdemir, A. V. Sumant, *Carbon* **2019**, *146*, 524.
- [85] A. V. Ayyagari, K. C. Mutyala, A. V. Sumant, *Sci. Rep.* **2020**, *10*, 15390.
- [86] a) B. Anasori, C. Shi, E. J. Moon, Y. Xie, C. A. Voigt, P. R. C. Kent, S. J. May, S. J. L. Billinge, M. W. Barsoum, Y. Gogotsi, *Nanoscale Horiz.* **2016**, *1*, 227; b) X. Yin, J. Jin, X. Chen, A. Rosenkranz, J. Luo, *ACS Appl. Mater. Interfaces* **2019**, *11*, 32569.
- [87] D. Berman, A. Erdemir, A. V. Sumant, *Carbon* **2013**, *54*, 454.
- [88] Y. Mai, H. Ling, F. Chen, C. Liu, L. Zhang, X. Jie, *Mater. Res. Bull.* **2018**, *102*, 324.
- [89] A. Vellore, S. Romero Garcia, N. Walters, D. A. Johnson, A. Kennett, M. Heverly, A. Martini, *Adv. Mater. Interfaces* **2020**, *7*, 2001109.
- [90] S. V. Prasad, J. S. Zabinski, N. T. McDevitt, *Tribol. Trans.* **1995**, *38*, 57.



- [91] S. Watanabe, J. Noshiro, S. Miyake, *Surf. Coat. Technol.* **2004**, *183*, 347.
- [92] M.-S. Won, O. V. Penkov, D.-E. Kim, *Carbon* **2013**, *54*, 472.
- [93] S. Qi, X. Li, H. Dong, *Mater. Lett.* **2017**, *209*, 15.
- [94] T. W. Scharf, P. G. Kotula, S. V. Prasad, *Acta Mater.* **2010**, *58*, 4100.
- [95] P. Li, P. Ju, L. Ji, H. Li, X. Liu, L. Chen, H. Zhou, J. Chen, *Adv. Mater.* **2020**, *32*, 2002039.
- [96] M. Marian, S. Tremmel, S. Wartzack, G. Song, B. Wang, J. Yu, A. Rosenkranz, *Appl. Surf. Sci.* **2020**, *523*, 146503.
- [97] Z. Ji, L. Zhang, G. Xie, W. Xu, D. Guo, J. Luo, B. Prakash, *Friction* **2020**, *8*, 813.
- [98] M. Dong, H. Zhang, L. Tzounis, G. Santagiuliana, E. Bilotti, D. G. Papageorgiou, *Carbon* **2021**, *185*, 57.
- [99] a) N. Jaya Prakash, B. Kandasubramanian, *J. Alloys Compd.* **2021**, *862*, 158547; b) V. N. Mochalin, Y. Gogotsi, *Diamond Relat. Mater.* **2015**, *58*, 161.
- [100] H. Zhang, L. Wang, Q. Chen, P. Li, A. Zhou, X. Cao, Q. Hu, *Mater. Des.* **2016**, *92*, 682.
- [101] a) H. Zhang, L. Wang, A. Zhou, C. Shen, Y. Dai, F. Liu, J. Chen, P. Li, Q. Hu, *RSC Adv.* **2016**, *6*, 87341; b) Y. Yang, G. Yang, K. Hou, H. Wang, N. Wang, S. Yang, J. Wang, *Carbon* **2021**, *184*, 12.
- [102] H. Yan, L. Zhang, H. Li, X. Fan, M. Zhu, *Carbon* **2020**, *157*, 217.
- [103] F. Meng, Z. Zhang, P. Gao, R. Kang, Y. Boyjoo, J. Yu, T. Liu, *Friction* **2020**, *9*, 734.
- [104] Y. Zhou, M. Liu, Y. Wang, J. Yuan, X. Men, *Tribol. Int.* **2022**, *165*, 108813.
- [105] C.-F. Du, Z. Wang, X. Wang, X. Zhao, J. Gao, Y. Xue, Y. Jiang, H. Yu, Q. Ye, *Tribol. Int.* **2022**, *165*, 107328.
- [106] Z. Xu, X. Shen, T. Wang, Y. Yang, J. Yi, M. Cao, J. Shen, Y. Xiao, J. Guan, X. Jiang, B. Tang, H. Li, *ACS Omega* **2021**, *6*, 29184.
- [107] H. Yan, J. Wang, C. Meng, X. Wang, S. Song, X. Fan, L. Zhang, H. Li, W. Li, M. Zhu, *Corros. Sci.* **2020**, *174*, 107314.
- [108] H. Yan, M. Cai, W. Li, X. Fan, M. Zhu, *J. Mater. Sci. Technol.* **2020**, *54*, 144.
- [109] L. Guo, Y. Zhang, G. Zhang, Q. Wang, T. Wang, *Tribol. Int.* **2021**, *153*, 106588.
- [110] Y. Zhang, X. He, M. Cao, X. Shen, Y. Yang, J. Yi, J. Guan, J. Shen, M. Xi, Y. Zhang, B. Tang, *Materials* **2021**, *14*, 2509.
- [111] B. C. Wyatt, S. K. Nemani, B. Anasori, *Nano Convergence* **2021**, *8*, 16.
- [112] Y. J. Mai, Y. G. Li, S. L. Li, L. Y. Zhang, C. S. Liu, X. H. Jie, *J. Alloys Compd.* **2019**, *770*, 1.
- [113] M. Li, S. Wang, Q. Wang, F. Ren, Y. Wang, *Mater. Sci. Eng., A* **2021**, *803*, 140699.
- [114] J. Hu, S. Li, J. Zhang, Q. Chang, W. Yu, Y. Zhou, *Chin. Chem. Lett.* **2020**, *31*, 996.
- [115] H. Guan, X. Lu, Q. Yao, Y. Wang, X. Liu, G. Xia, D. Zhao, *Ceram. Int.* **2022**, *48*, 1926.
- [116] a) L. Liu, G. Ying, C. Hu, K. Zhang, F. Ma, L. Su, C. Zhang, C. Wang, *ACS Appl. Nano Mater.* **2019**, *2*, 5553; b) L. Liu, G. Ying, D. Wen, K. Zhang, C. Hu, Y. Zheng, C. Zhang, X. Wang, C. Wang, *Mater. Des.* **2021**, *197*, 109276.
- [117] a) F. Zhang, W. Liu, S. Wang, C. Liu, H. Shi, L. Liang, K. Pi, *Composites, Part B* **2021**, *217*, 108900; b) S. Li, H. Huang, F. Chen, X. He, Y. Ma, L. Zhang, X. Sheng, Y. Chen, E. Shchukina, D. Shchukin, *Prog. Org. Coat.* **2021**, *161*, 106478.
- [118] J. T. Lee, B. C. Wyatt, G. A. Davis, Jr., A. N. Masterson, A. L. Pagan, A. Shah, B. Anasori, R. Sardar, *ACS Nano* **2021**, *15*, 19600.
- [119] C. Qu, S. Li, Y. Zhang, T. Wang, Q. Wang, S. Chen, *Tribol. Int.* **2021**, *163*, 107150.
- [120] Y. Guo, X. Zhou, D. Wang, X. Xu, Q. Xu, *Langmuir* **2019**, *35*, 14481.
- [121] Y. Guan, M. Zhang, J. Qin, X. Ma, C. Li, J. Tang, *J. Phys. Chem. C* **2020**, *124*, 13664.
- [122] A. Rodriguez, M. S. Jaman, O. Acikgoz, B. Wang, J. Yu, P. G. Grützmacher, A. Rosenkranz, M. Z. Baykara, *Appl. Surf. Sci.* **2021**, *535*, 147664.
- [123] X. Zhou, Y. Guo, D. Wang, Q. Xu, *Tribol. Int.* **2021**, *153*, 106646.
- [124] a) P. Serles, M. Hamidinejad, P. G. Demingos, L. Ma, N. Barri, H. Taylor, C. V. Singh, C. B. Park, T. Filleter, *Nano Lett.* **2022**, *22*, 3356; b) C. Lee, Q. Li, W. Kalb, X. Z. Liu, H. Berger, R. W. Carpick, J. Hone, *Science* **2010**, *328*, 76.
- [125] A. Kozak, M. Hofbauerova, Y. Halahovets, L. Pribusova-Slusna, M. Precner, M. Micusik, L. Orovcik, M. Hulman, A. Stepura, M. Omastova, P. Siffalovic, M. Tapajna, *ACS Appl. Mater. Interfaces* **2022**, *14*, 36815.
- [126] H. Zhang, Z. H. Fu, D. Legut, T. C. Germann, R. F. Zhang, *RSC Adv.* **2017**, *7*, 55912.
- [127] D. Zhang, M. Ashton, A. Ostadhossein, A. C. T. van Duin, R. G. Hennig, S. B. Sinnott, *ACS Appl. Mater. Interfaces* **2017**, *9*, 34467.
- [128] a) S. Curtarolo, G. L. W. Hart, M. B. Nardelli, N. Mingo, S. Sanvito, O. Levy, *Nat. Mater.* **2013**, *12*, 191; b) G. Hautier, A. Jain, S. P. Ong, *J. Mater. Sci.* **2012**, *47*, 7317.
- [129] E. Marquis, M. Cutini, B. Anasori, A. Rosenkranz, M. C. Righi, *ACS Appl. Nano Mater.* **2022**, *5*, 10516.
- [130] P. Restuccia, G. Levita, M. Wolloch, G. Losi, G. Fatti, M. Ferrario, M. C. Righi, *Comput. Mater. Sci.* **2018**, *154*, 517.
- [131] M. Wolloch, G. Losi, M. Ferrario, M. C. Righi, *Sci. Rep.* **2019**, *9*, 17062.
- [132] M. Wolloch, G. Levita, P. Restuccia, M. C. Righi, *Phys. Rev. Lett.* **2018**, *121*, 026804.
- [133] B. Sattari Baboukani, Z. Ye, K. G. Reyes, P. C. Nalam, *Tribol. Lett.* **2020**, *68*, 57.
- [134] a) G. Levita, M. C. Righi, *ChemPhysChem* **2017**, *18*, 1475; b) M. Stella, C. D. Lorenz, M. C. Righi, *2D Mater.* **2021**, *8*, 035052; c) P. Restuccia, M. Ferrario, M. C. Righi, *Carbon* **2020**, *156*, 93.
- [135] P. Restuccia, M. C. Righi, *Carbon* **2016**, *106*, 118.
- [136] A. Rosenkranz, M. Marian, F. J. Profito, N. Aragon, R. Shah, *Lubricants* **2021**, *9*, 2.
- [137] M. Marian, S. Tremmel, *Lubricants* **2021**, *9*, 86.
- [138] A. Rosenkranz, M. Marian, *Surf. Topogr.: Metrol. Prop.* **2022**, *3*, 10.
- [139] a) Y. Xue, X. Shi, Q. Huang, K. Zhang, C. Wu, *Tribol. Int.* **2021**, *161*, 107099; b) Y. Xue, C. Wu, X. Shi, K. Zhang, Q. Huang, *Tribol. Int.* **2021**, *164*, 107205.
- [140] Q. Huang, X. Shi, J. Ma, *J. Mater. Eng. Perform.* **2021**, *30*, 9390.
- [141] Y. Dong, S. S. K. Mallineni, K. Maleski, H. Behlow, V. N. Mochalin, A. M. Rao, Y. Gogotsi, R. Podila, *Nano Energy* **2018**, *44*, 103.



**Andreas Rosenkranz** is a professor for Material-Oriented Tribology and New 2D Materials in the Department of Chemical Engineering, Biotechnology and Materials at the University of Chile. His research focuses on the characterization, chemical functionalization, and application of 2D materials. His main field of research relates to tribology, but, recently, he has also expanded his fields toward water purification, catalysis, and biological properties. He has published more than 140 peer-reviewed journal publications, is a fellow of the Alexander von Humboldt Foundation, and acts as a scientific editor for journals including *Applied Nanoscience* and *Frontiers of Chemistry*.



**M. Clelia Righi** is full professor at the Physics Department of Bologna University, Italy. Her research focuses on the development and application of computational tools to design materials and describe their function in operando conditions. She adopted pioneering approaches in computational tribology to study lubricant additives, solid lubricants, and coatings. She has long-standing collaborations with multinational industries operating in the energy, semiconductor, and automotive sectors. In 2019, she received an ERC consolidator grant for the project “Advancing solid interfaces and lubricants by first principles material design”. She is part of the editorial boards of *Lubricants*, *Lubrication Science*, and *Scientific Reports*.



**Anirudha Sumant** is a group leader, Nanofabrication and Devices Group and Materials scientist at the Center for Nanoscale Materials, Argonne National Laboratory, and leading the research on tribological and electronic properties of nanocarbon materials. His recent work on demonstrating superlubricity (near zero friction) at engineering scale utilizing 2D materials opened a new era in solid lubrication technology. He is the author and co-author of more than 150 peer-reviewed journal/proceedings publications, 2 book chapters, and has 36 granted patents. He is a chief specialty editor of the journal *Frontiers in Carbon* and advisory board member of *Applied Physics Letters*.



**Babak Anasori** is an assistant professor at the Purdue School of Engineering and Technology, Indiana University–Purdue University Indianapolis. He received his Ph.D. in materials science and engineering from Drexel University in 2014. He is one of the inventors of ordered double-transition metal MXenes and high-entropy MXenes. He has co-authored more than 145 journal papers and co-edited the first book on MXenes in 2019. He is among the Web of Science Highly Cited Researchers in 2019, 2020, and 2021. His lab works on the synthesis and characterizations of novel MXenes and their composites, mechanical, and electrocatalysis properties.



**Vadym Mochalin** holds a Ph.D. in physical chemistry from L. M. Litvinenko Institute of Physical Organic and Coal Chemistry, National Academy of Sciences of Ukraine. He is Associate Professor in chemistry at Missouri University of Science and Technology with joint appointment in the Department of Materials Science and Engineering. His research concerns synthesis, characterization, purification, modification, modeling, and applications of nanodiamond, MXenes, other nanomaterials for composites, energy storage, biomedicine, and optoelectronics. He has co-authored many research papers, several book chapters and reviews, and is an inventor on 7 international patents. Editor in *Scientific Reports* and *Diamond and Related Materials*.